

Baryon Asymmetry, Neutrino Mixing and Supersymmetric SO(10) Unification

Michael Plümacher*

Deutsches Elektronen-Synchrotron DESY,
Notkestr. 85, D-22603 Hamburg, Germany

Abstract

The baryon asymmetry of the universe can be explained by the out-of-equilibrium decays of heavy right-handed neutrinos. We analyse this mechanism in the framework of a supersymmetric extension of the Standard Model and show that lepton number violating scatterings are indispensable for baryogenesis, even though they may wash-out a generated asymmetry. By assuming a similar pattern of mixings and masses for neutrinos and up-type quarks, as suggested by SO(10) unification, we can generate the observed baryon asymmetry without any fine tuning, if $(B - L)$ is broken at the unification scale $\Lambda_{\text{GUT}} \sim 10^{16}$ GeV and, if $m_{\nu_\mu} \sim 3 \cdot 10^{-3}$ eV as preferred by the MSW solution to the solar neutrino deficit.

*e-mail: pluemi@mail.desy.de

1 Introduction

The observed baryon asymmetry of the universe

$$Y_B = \frac{n_B}{s} = (0.6 - 1) \cdot 10^{-10}, \quad (1)$$

cannot be explained within the Standard Model, i.e. one has to envisage extensions of the Standard Model. Grand unified theories (GUTs) are attractive for various reasons and there have been many attempts to generate Y_B at the GUT scale [1]. However, these mechanisms seem to be incompatible with inflationary scenarios which require reheating temperatures well below the GUT scale, the influence of preheating [2] on the baryon asymmetry requiring further studies.

During the evolution of the early universe, the electroweak phase transition is the last opportunity to generate a baryon asymmetry without being in conflict with the strong experimental bounds on baryon number violation at low energies [3]. However, the thermodynamics of this transition indicates that such scenarios are rather unlikely [4].

Therefore, the baryon asymmetry has to be generated between the reheating scale and the electroweak scale, where baryon plus lepton number ($B + L$) violating anomalous processes are in thermal equilibrium [5], thereby making a ($B - L$) violation necessary for baryogenesis. Hence, no asymmetry can be generated within GUT scenarios based on the gauge group SU(5), where ($B - L$) is a conserved quantity.

Gauge groups containing SO(10) predict the existence of right-handed neutrinos. In such theories ($B - L$) is spontaneously broken, one consequence being that the right-handed neutrinos can acquire a large Majorana mass, thereby explaining the smallness of the light neutrino masses via the see-saw mechanism [6]. Heavy right-handed Majorana neutrinos violate lepton number in their decays, thus implementing the required ($B - L$) breaking as lepton number violation. This leptogenesis mechanism was first suggested by Fukugita and Yanagida [7] and has subsequently been studied by several authors [8–13].

If one assumes a similar pattern of mass ratios and mixings for leptons and quarks and, if $m_{\nu_\mu} \sim 3 \cdot 10^{-3}$ eV as preferred by the MSW solution to the solar neutrino problem, leptogenesis implies that ($B - L$) is broken at the unification scale [12]. This suggests a grand unified theory based on the group SO(10), or one of its extensions, which is directly broken into the Standard Model gauge group at the unification scale $\sim 10^{16}$ GeV. However, for a successful gauge coupling unification, such a GUT scenario requires low-energy supersymmetry.

Supersymmetric leptogenesis has already been considered in refs. [10,13] in the approximation that there are no lepton number violating scatterings which can inhibit the generation of a lepton number. Another usually neglected problem of leptogenesis scenarios is the necessary production of the right-handed neutrinos after reheating. In the non-supersymmetric scenarios one has to assume additional interactions of the right-handed neutrinos for successful leptogenesis [11].

In this paper, we investigate supersymmetric leptogenesis within the framework of the minimal supersymmetric standard model (MSSM) to which we add right-handed Majorana neutrinos, as suggested by SO(10) unification. In the next section we will discuss the neutrino decays and scattering processes that one has to take into account to be consistent. In section 3 we will develop the full network of Boltzmann equations necessary to get a reliable relation between the input parameters and the final baryon asymmetry. We will show that by neglecting the lepton number violating scatterings one largely overestimates the generated asymmetry and that in our scenario the Yukawa interactions are strong enough to produce a thermal population of right-handed neutrinos at high temperatures. Finally we will see in section 4 that by assuming a similar pattern of masses and mixings for leptons and quarks one gets the required value for the baryon asymmetry without any fine tuning, provided $(B - L)$ is broken at the GUT scale and the Dirac mass scale for the neutrinos is of order of the top-quark mass, as suggested by SO(10) unification.

In the appendices A and B we introduce our notations concerning superfields and the Boltzmann equations, respectively. The reduced cross sections for the scattering processes discussed in section 2 can be found in appendix C, while appendix D summarizes some limiting cases in which the corresponding reaction densities can be calculated analytically.

2 The model

2.1 The superpotential

In supersymmetric unification scenarios based on SO(10), the effective theory below the $(B - L)$ breaking scale is the MSSM supplemented by right-handed Majorana neutrinos. Neglecting soft breaking terms, the masses and Yukawa couplings relevant for leptogenesis are given by the superpotential

$$\mathcal{W} = \frac{1}{2} N^c M N^c + \mu H_1 \epsilon H_2 + H_1 \epsilon Q \lambda_d D^c + H_1 \epsilon L \lambda_l E^c + H_2 \epsilon Q \lambda_u U^c + H_2 \epsilon L \lambda_\nu N^c, \quad (2)$$

where we have chosen a basis in which the Majorana mass matrix M and the Yukawa coupling matrices λ_d and λ_l for the down-type quarks and the charged leptons are diagonal with real and positive eigenvalues.

The vacuum expectation values of the neutral Higgs fields generate Dirac masses for the down-type quarks and the charged leptons

$$v_1 = \langle H_1 \rangle \neq 0 \quad \Rightarrow \quad m_d = \lambda_d v_1 \quad \text{and} \quad m_l = \lambda_l v_1, \quad (3)$$

and for the up-type quarks and the neutrinos

$$v_2 = \langle H_2 \rangle \neq 0 \quad \Rightarrow \quad m_u = \lambda_u v_2 \quad \text{and} \quad m_D = \lambda_\nu v_2. \quad (4)$$

The Majorana masses M for the right-handed neutrinos, which have to be much larger than the Dirac masses m_D , offer a natural explanation for the smallness of the light neutrino masses via the see-saw mechanism [6].

To get a non-vanishing lepton asymmetry, one needs non-degenerate Majorana masses M_i . Then the scale at which the asymmetry is generated is given by the mass M_1 of the lightest right-handed neutrino. Hence, it is convenient to write all the masses and energies in units of M_1 ,

$$a_j := \left(\frac{M_j}{M_1}\right)^2, \quad x = \frac{s}{M_1^2} \quad \text{and} \quad z = \frac{M_1}{T}, \quad (5)$$

where M_j are the masses of the heavier right-handed neutrinos, s is the squared centre of mass energy of a scattering process and T is the temperature.

2.2 The decay channels of the heavy neutrinos

The right-handed Majorana neutrinos N_j can decay into a lepton and a Higgs boson or into a slepton and a higgsino, while their scalar partners \widetilde{N}_j^c can decay into a lepton and a higgsino or into a slepton and a Higgs boson (cf. fig. 1). The decay widths at tree level read [13]

$$\begin{aligned} \frac{1}{4}\Gamma_{N_j} &:= \Gamma(N_j \rightarrow \tilde{l} + \bar{h}) = \Gamma(N_j \rightarrow \tilde{l}^\dagger + \tilde{h}) \\ &= \Gamma(N_j \rightarrow l + H_2) = \Gamma(N_j \rightarrow \bar{l} + H_2^\dagger) = \frac{M_j}{16\pi} \frac{(m_D^\dagger m_D)_{jj}}{v_2^2}, \end{aligned} \quad (6)$$

$$\begin{aligned} \frac{1}{2}\Gamma_{N_j}^{(2)} &:= \Gamma(\widetilde{N}_j^c \rightarrow \tilde{l} + H_2) = \Gamma(\widetilde{N}_j^c \rightarrow \bar{l} + \tilde{h}) \\ &= \Gamma(\widetilde{N}_j^{c\dagger} \rightarrow \tilde{l}^\dagger + H_2^\dagger) = \Gamma(\widetilde{N}_j^{c\dagger} \rightarrow l + \bar{h}) = \frac{M_j}{8\pi} \frac{(m_D^\dagger m_D)_{jj}}{v_2^2}. \end{aligned} \quad (7)$$

According to eq. (B.5), the reaction densities for these decays are then given by

$$\gamma_{N_j} = 2 \gamma_{N_j^{(2)}}^{(2)} = \frac{M_1^4}{4\pi^3} \frac{(m_D^\dagger m_D)_{jj}}{v_2^2} \frac{a_j \sqrt{a_j}}{z} \text{K}_1(z\sqrt{a_j}). \quad (8)$$

All these decay modes are CP violating, the dominant contribution to CP violation coming about through interference between the tree level and the one-loop diagrams shown in fig. 1. The CP asymmetries in the different decay channels of N_j and \widetilde{N}_j^c can all be expressed by the same CP violation parameter ε_j ,

$$\begin{aligned} \varepsilon_j &:= \frac{\Gamma(N_j \rightarrow \tilde{l} + \bar{h}) - \Gamma(N_j \rightarrow \tilde{l}^\dagger + \tilde{h})}{\Gamma(N_j \rightarrow \tilde{l} + \bar{h}) + \Gamma(N_j \rightarrow \tilde{l}^\dagger + \tilde{h})} = \frac{\Gamma(N_j \rightarrow l + H_2) - \Gamma(N_j \rightarrow \bar{l} + H_2^\dagger)}{\Gamma(N_j \rightarrow l + H_2) + \Gamma(N_j \rightarrow \bar{l} + H_2^\dagger)} \\ &= \frac{\Gamma(\widetilde{N}_j^{c\dagger} \rightarrow l + \bar{h}) - \Gamma(\widetilde{N}_j^c \rightarrow \bar{l} + \tilde{h})}{\Gamma(\widetilde{N}_j^{c\dagger} \rightarrow l + \bar{h}) + \Gamma(\widetilde{N}_j^c \rightarrow \bar{l} + \tilde{h})} = \frac{\Gamma(\widetilde{N}_j^c \rightarrow \tilde{l} + H_2) - \Gamma(\widetilde{N}_j^{c\dagger} \rightarrow \tilde{l}^\dagger + H_2^\dagger)}{\Gamma(\widetilde{N}_j^c \rightarrow \tilde{l} + H_2) + \Gamma(\widetilde{N}_j^{c\dagger} \rightarrow \tilde{l}^\dagger + H_2^\dagger)} \end{aligned}$$

$$= -\frac{1}{8\pi v_2^2} \frac{1}{(m_D^\dagger m_D)_{jj}} \sum_{n \neq j} \text{Im} [(m_D^\dagger m_D)_{nj}^2] g\left(\frac{a_n}{a_j}\right), \quad (9)$$

$$\text{with } g(x) = \sqrt{x} \left[\ln\left(\frac{1+x}{x}\right) + \frac{2}{x-1} \right] \approx \frac{3}{\sqrt{x}} \text{ for } x \gg 1.$$

Here n is the flavour index of the intermediate heavy (s)neutrino. This result agrees with the one in ref. [13] and is of the same order as the CP asymmetry in ref. [10].

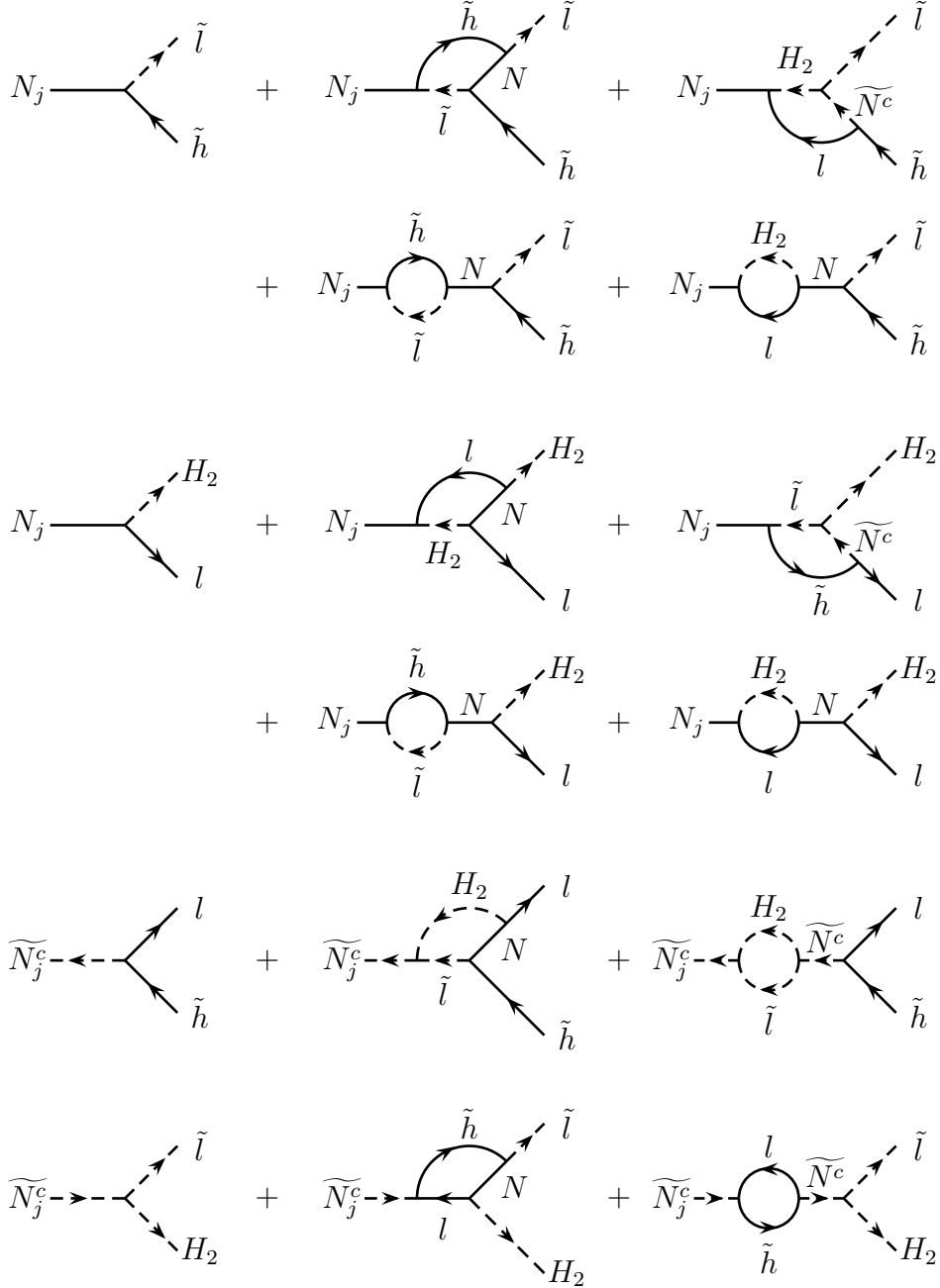


Figure 1: *Decay modes of the right-handed Majorana neutrinos and their scalar partners.*

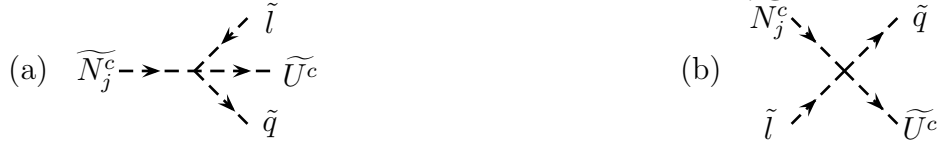


Figure 2: Contributions of the scalar potential to the decay width and the interactions of a scalar neutrino.

With ε_j we can parametrize the reaction densities for the decays and inverse decays in the following way

$$\begin{aligned}
\gamma(N_j \rightarrow \tilde{l} + \tilde{h}) &= \gamma(N_j \rightarrow l + H_2) = \gamma(\tilde{l}^\dagger + \tilde{h} \rightarrow N_j) = \gamma(\tilde{l} + H_2^\dagger \rightarrow N_j) = \frac{1}{4}(1 + \varepsilon_j)\gamma_{N_j} \\
\gamma(N_j \rightarrow \tilde{l}^\dagger + \tilde{h}) &= \gamma(N_j \rightarrow \bar{l} + H_2^\dagger) = \gamma(\tilde{l} + \tilde{h} \rightarrow N_j) = \gamma(l + H_2 \rightarrow N_j) = \frac{1}{4}(1 - \varepsilon_j)\gamma_{N_j} \\
\gamma(\widetilde{N}_j^c \rightarrow \tilde{l} + H_2) &= \gamma(\widetilde{N}_j^{c\dagger} \rightarrow l + \tilde{h}) = \gamma(\tilde{l}^\dagger + H_2^\dagger \rightarrow \widetilde{N}_j^{c\dagger}) = \gamma(\tilde{l} + \tilde{h} \rightarrow \widetilde{N}_j^c) = \frac{1}{2}(1 + \varepsilon_j)\gamma_{\widetilde{N}_j^c}^{(2)} \\
\gamma(\widetilde{N}_j^{c\dagger} \rightarrow \tilde{l}^\dagger + H_2^\dagger) &= \gamma(\widetilde{N}_j^c \rightarrow \bar{l} + \tilde{h}) = \gamma(\tilde{l} + H_2 \rightarrow \widetilde{N}_j^c) = \gamma(l + \tilde{h} \rightarrow \widetilde{N}_j^{c\dagger}) = \frac{1}{2}(1 - \varepsilon_j)\gamma_{\widetilde{N}_j^c}^{(2)}
\end{aligned}$$

Additionally, the scalar potential contains quartic scalar couplings, which enable the decay of \widetilde{N}_j^c into three particles via the diagram shown in fig. 2a. The partial width for this decay is given by

$$\Gamma_{\widetilde{N}_j^c}^{(3)} := \Gamma(\widetilde{N}_j^{c\dagger} \rightarrow \tilde{l} + \widetilde{U}^{c\dagger} + \tilde{q}^\dagger) = \frac{3\alpha_u M_j}{64\pi^2} \frac{(m_D^\dagger m_D)_{jj}}{v_2^2} \quad \text{with} \quad \alpha_u = \frac{\text{Tr}(\lambda_u^\dagger \lambda_u)}{4\pi}, \quad (10)$$

and the corresponding reaction density reads

$$\gamma_{\widetilde{N}_j^c}^{(3)} = \frac{3\alpha_u M_1^4}{128\pi^4} \frac{(m_D^\dagger m_D)_{jj}}{v_2^2} \frac{a_j \sqrt{a_j}}{z} \text{K}_1(z\sqrt{a_j}) = \frac{3\alpha_u}{16\pi} \gamma_{\widetilde{N}_j^c}^{(2)}. \quad (11)$$

Since the Yukawa coupling of the top quark and its scalar partner is large, α_u can be of order one. But even then $\gamma_{\widetilde{N}_j^c}^{(3)}$ is much smaller than $\gamma_{\widetilde{N}_j^c}^{(2)}$. Hence, the three particle decays give only a small correction, which we have taken into account for completeness. However, we have neglected the CP asymmetry in this decay which comes about through similar one-loop diagrams as in fig. 1.

The dimensionless squared total decay widths of N_j and \widetilde{N}_j^c are then finally given by

$$c_j := \left(\frac{\Gamma_{N_j}}{M_1} \right)^2 = \frac{a_j}{16\pi^2} \frac{(m_D^\dagger m_D)_{jj}^2}{v_2^4}, \quad (12)$$

$$\tilde{c}_j := \left(\frac{\Gamma_{\widetilde{N}_j^c}^{(2)} + \Gamma_{\widetilde{N}_j^c}^{(3)}}{M_1} \right)^2 = \frac{a_j}{16\pi^2} \frac{(m_D^\dagger m_D)_{jj}^2}{v_2^4} \left[1 + \frac{3\alpha_u}{16\pi} \right]^2. \quad (13)$$

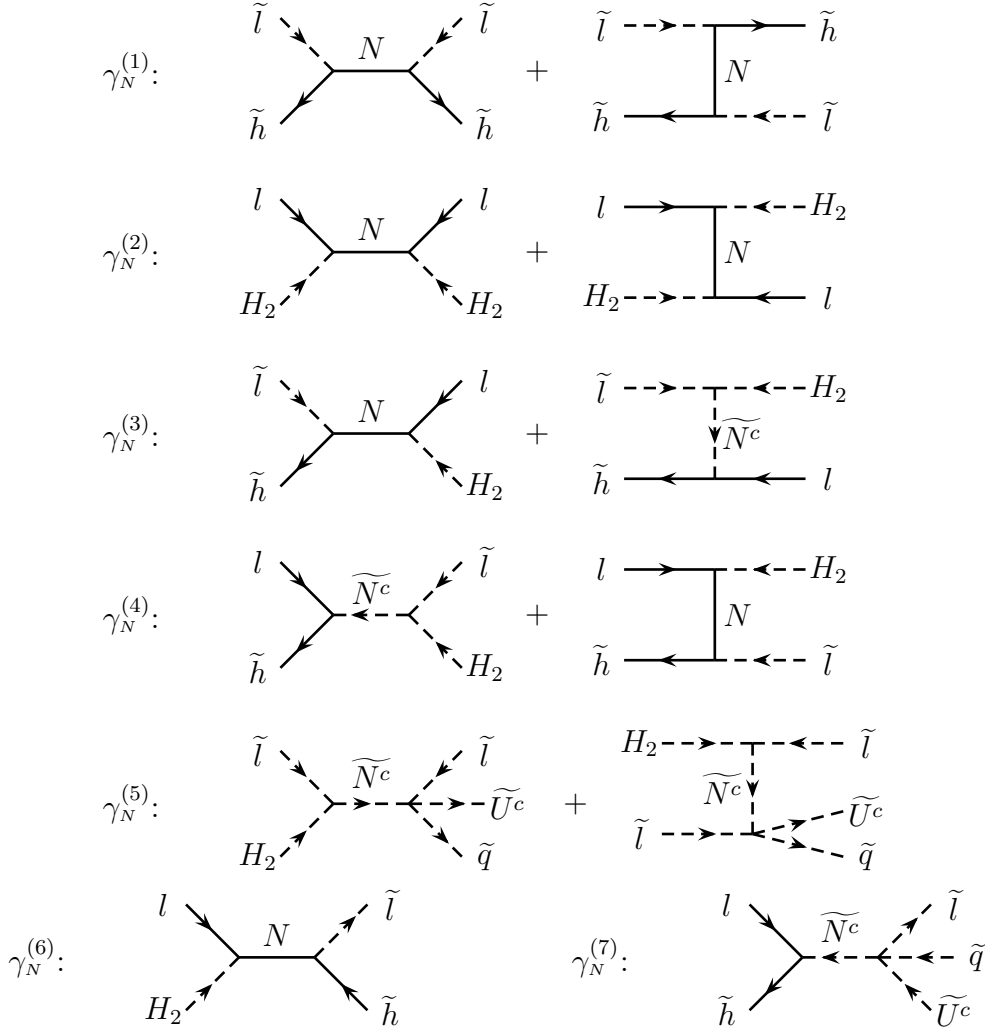


Figure 3: L violating processes mediated by a virtual Majorana neutrino or its scalar partner.

The vertex in fig. 2a also gives $2 \rightarrow 2$ scattering processes involving one scalar neutrino, like $\widetilde{N}_j^c + \tilde{l} \rightarrow \tilde{q} + \widetilde{U}^c$ (cf. fig. 2b). The reduced cross section for this process reads

$$\hat{\sigma}_{22_j}(x) = 3\alpha_u \frac{(m_D^\dagger m_D)_{jj}}{v_2^2} \frac{x - a_j}{x}. \quad (14)$$

For the processes $\widetilde{N}_j^c + \tilde{q}^\dagger \rightarrow \tilde{l}^\dagger + \widetilde{U}^c$ and $\widetilde{N}_j^c + \widetilde{U}^{\dagger c} \rightarrow \tilde{l}^\dagger + \tilde{q}$, the corresponding back reactions and the CP conjugated processes we find the same result. The corresponding reaction density can then be calculated according to eq. (B.6). One finds

$$\gamma_{22_j}(z) = \frac{3\alpha_u M_1^4}{16\pi^4} \frac{(m_D^\dagger m_D)_{jj}}{v_2^2} \frac{\sqrt{a_j}}{z^3} K_1(z\sqrt{a_j}) = \frac{3\alpha_u}{4\pi a_j z^2} \gamma_{N_j}(z). \quad (15)$$

Hence, γ_{22_j} will be much larger than γ_{N_j} for small $a_j z^2$, i.e. for high temperatures $T \gg M_j$. Together with similar scatterings which we are going to discuss in section 2.4, these processes will therefore be very effective in bringing the heavy (s)neutrinos into thermal equilibrium at high temperatures where decays and inverse decays are suppressed by a time dilatation factor.

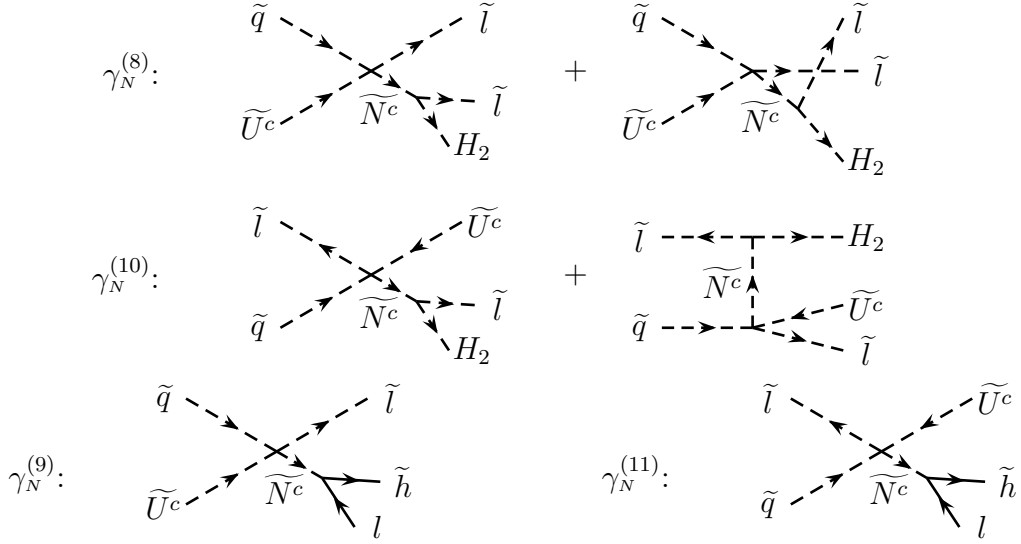


Figure 4: *Diagrams contributing to the lepton number violating scatterings via heavy sneutrino exchange.*

2.3 Lepton number violating scatterings mediated by the right-handed neutrinos

Using the tree level vertices from figs. 1 and 2 as building blocks we can construct lepton number violating scatterings mediated by a heavy (s)neutrino. Although of higher order than the tree level decays, these diagrams have to be taken into consideration to avoid the generation of an asymmetry in thermal equilibrium (cf. ref. [14]). In this section we will only mention the different processes which have to be considered. The corresponding reduced cross sections can be found in appendix C and the reaction densities are discussed in appendix D.

By combining two of the decay vertices (cf. fig. 1 and fig. 2a) one gets the processes that we have shown in fig. 3 and the corresponding CP conjugated processes. We will use the following abbreviations for the reaction densities

$$\begin{aligned}
\gamma_N^{(1)} &= \gamma(\tilde{l} + \bar{\tilde{h}} \leftrightarrow \tilde{l}^\dagger + \tilde{h}) , & \gamma_N^{(2)} &= \gamma(l + H_2 \leftrightarrow \bar{l} + H_2^\dagger) , \\
\gamma_N^{(3)} &= \gamma(\tilde{l} + \bar{\tilde{h}} \leftrightarrow \bar{l} + H_2^\dagger) , & \gamma_N^{(4)} &= \gamma(l + \bar{\tilde{h}} \leftrightarrow \tilde{l}^\dagger + H_2^\dagger) , \\
\gamma_N^{(5)} &= \gamma(\tilde{l} + H_2 \leftrightarrow \tilde{l}^\dagger + \tilde{U}^c + \tilde{q}) , & \gamma_N^{(6)} &= \gamma(l + H_2 \leftrightarrow \bar{l} + \bar{\tilde{h}}) , \\
\gamma_N^{(7)} &= \gamma(l + \bar{\tilde{h}} \leftrightarrow \tilde{l} + \tilde{q}^\dagger + \tilde{U}^{c\dagger}) .
\end{aligned}$$

The contributions from on-shell (s)neutrinos contained in these reactions have already been taken into account as inverse decay followed by a decay. Hence, one has to subtract the contributions from real intermediate states to avoid a double counting of reactions [14].

From the scattering vertex in fig. 2b and the decay vertices we can construct the following processes

$$\begin{aligned}
\gamma_N^{(8)} &= \gamma(\widetilde{U}^c + \tilde{q} \leftrightarrow \tilde{l} + \tilde{l} + H_2), & \gamma_N^{(9)} &= \gamma(\tilde{q} + \widetilde{U}^c \leftrightarrow \tilde{l} + \bar{l} + \tilde{h}), \\
\gamma_N^{(10)} &= \gamma(\tilde{l}^\dagger + \tilde{q} \leftrightarrow \tilde{l} + \widetilde{U}^{c\dagger} + H_2) = \gamma(\tilde{l}^\dagger + \widetilde{U}^c \leftrightarrow \tilde{l} + \tilde{q}^\dagger + H_2), \\
\gamma_N^{(11)} &= \gamma(\tilde{l}^\dagger + \tilde{q} \leftrightarrow \bar{l} + \tilde{h} + \widetilde{U}^{c\dagger}) = \gamma(\tilde{l}^\dagger + \widetilde{U}^c \leftrightarrow \bar{l} + \tilde{h} + \tilde{q}^\dagger).
\end{aligned}$$

In fig. 4 we have shown one typical diagram for each of these reaction densities. Again, these diagrams have on-shell contributions which have to be subtracted, since they can be described as decay of a sneutrino which has been produced in a scattering process.

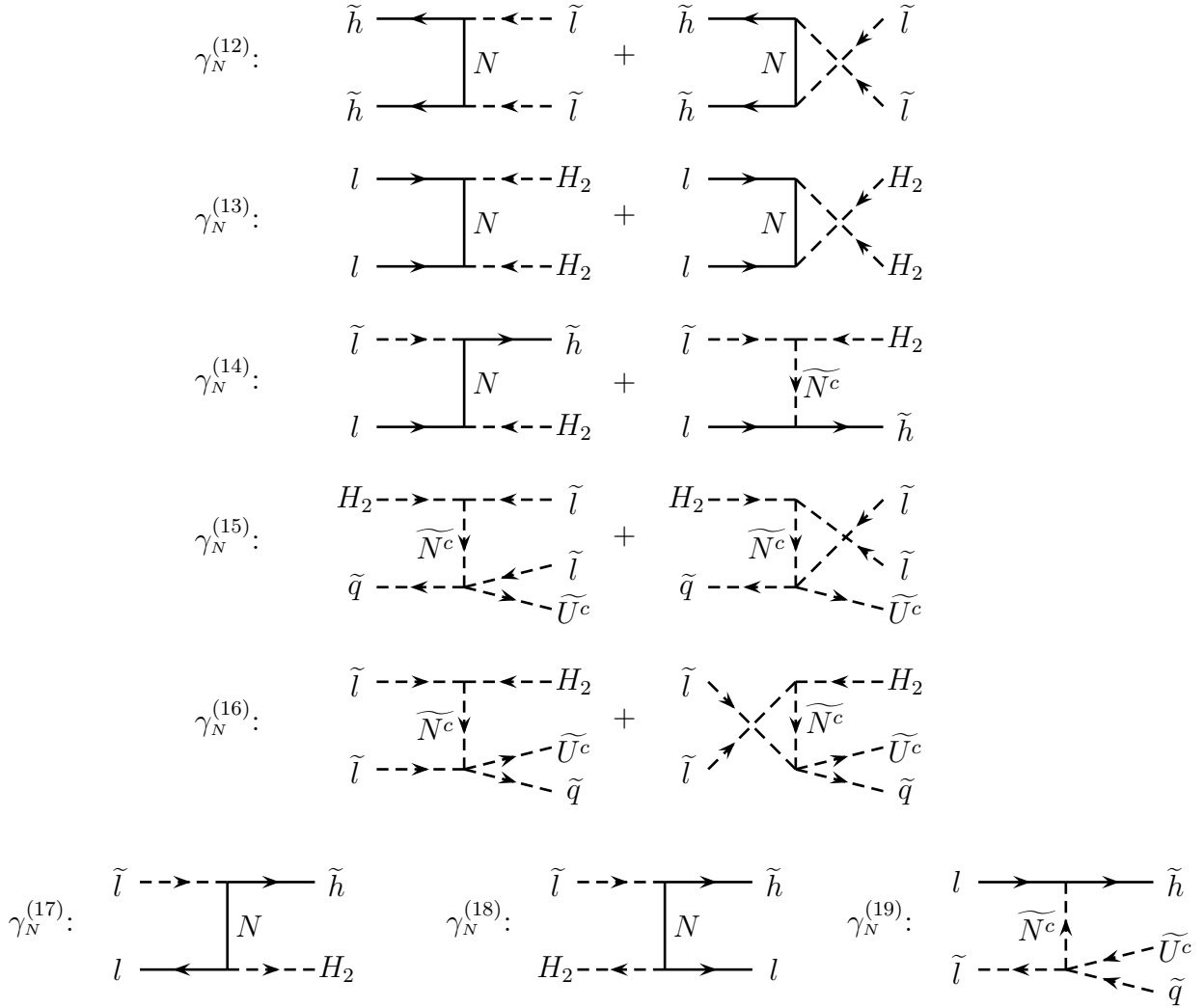


Figure 5: L violating processes mediated by a virtual Majorana neutrino in the t -channel.

Up to now we have only considered processes with a neutrino or its scalar partner in the s -channel. In fig. 5 we have shown a selection of diagrams without on-shell contributions. The corresponding reaction densities will be denoted by

$$\begin{aligned}
\gamma_N^{(12)} &= \gamma(\tilde{h} + \tilde{h} \leftrightarrow \tilde{l}^\dagger + \tilde{l}^\dagger), & \gamma_N^{(13)} &= \gamma(l + l \leftrightarrow H_2^\dagger + H_2^\dagger), \\
\gamma_N^{(14)} &= \gamma(\tilde{l} + l \leftrightarrow \tilde{h} + H_2^\dagger), & \gamma_N^{(16)} &= \gamma(\tilde{l} + \tilde{l} \leftrightarrow \widetilde{U}^c + \tilde{q} + H_2^\dagger),
\end{aligned}$$

$$\begin{aligned}
\gamma_N^{(15)} &= \gamma(H_2 + \tilde{q}^\dagger \leftrightarrow \tilde{l}^\dagger + \tilde{l}^\dagger + \tilde{U}^c) = \gamma(H_2 + \tilde{U}^{c\dagger} \leftrightarrow \tilde{l}^\dagger + \tilde{l}^\dagger + \tilde{q}), \\
\gamma_N^{(17)} &= \gamma(\tilde{l} + \bar{l} \leftrightarrow \tilde{h} + H_2), \quad \gamma_N^{(18)} = \gamma(\tilde{l} + H_2^\dagger \leftrightarrow \tilde{h} + l), \\
\gamma_N^{(19)} &= \gamma(l + \tilde{l}^\dagger \leftrightarrow \tilde{h} + \tilde{q}^\dagger + \tilde{U}^{c\dagger}) = \gamma(l + \tilde{q} \leftrightarrow \tilde{l} + \tilde{U}^{c\dagger} + \tilde{h}) \\
&= \gamma(l + \tilde{U}^c \leftrightarrow \tilde{l} + \tilde{q}^\dagger + \tilde{h}) = \gamma(\tilde{l}^\dagger + \tilde{h} \leftrightarrow \tilde{l} + \tilde{q}^\dagger + \tilde{U}^{c\dagger}) \\
&= \gamma(\tilde{q} + \tilde{h} \leftrightarrow \tilde{l} + \tilde{l} + \tilde{U}^{c\dagger}) = \gamma(\tilde{U}^c + \tilde{h} \leftrightarrow \tilde{l} + \tilde{l} + \tilde{q}^\dagger).
\end{aligned}$$

At first sight one may think that these diagrams could be neglected, since they are suppressed at intermediate temperatures, i.e. intermediate energies $x \approx a_j$. However, they give an important contribution to the effective lepton number violating interactions at low energies and therefore have to be taken into consideration.

2.4 Interactions with a top or a stop

The Yukawa coupling of the top quark is large. Thus we have to consider the lepton number violating interactions of a right-handed neutrino with a top quark or its scalar partner.

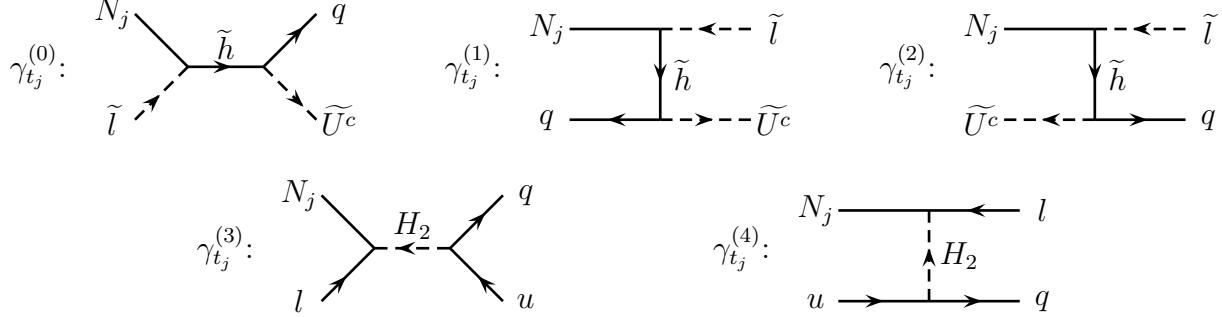


Figure 6: *Neutrino-(s)top scattering.*

For the neutrino we have to take into account the following processes (cf. fig. 6)

$$\begin{aligned}
\gamma_{t_j}^{(0)} &= \gamma(N_j + \tilde{l} \leftrightarrow q + \tilde{U}^c) = \gamma(N_j + \tilde{l} \leftrightarrow \tilde{q} + \bar{u}), \\
\gamma_{t_j}^{(1)} &= \gamma(N_j + \bar{q} \leftrightarrow \tilde{l}^\dagger + \tilde{U}^c) = \gamma(N_j + u \leftrightarrow \tilde{l}^\dagger + \tilde{q}), \\
\gamma_{t_j}^{(2)} &= \gamma(N_j + \tilde{U}^{c\dagger} \leftrightarrow \tilde{l}^\dagger + q) = \gamma(N_j + \tilde{q}^\dagger \leftrightarrow \tilde{l}^\dagger + \bar{u}), \\
\gamma_{t_j}^{(3)} &= \gamma(N_j + l \leftrightarrow q + \bar{u}), \\
\gamma_{t_j}^{(4)} &= \gamma(N_j + u \leftrightarrow \bar{l} + q) = \gamma(N_j + \bar{q} \leftrightarrow \bar{l} + \bar{u}).
\end{aligned}$$

At this order of perturbation theory these processes are CP invariant. Hence, we have the same reaction densities for the CP conjugated processes.

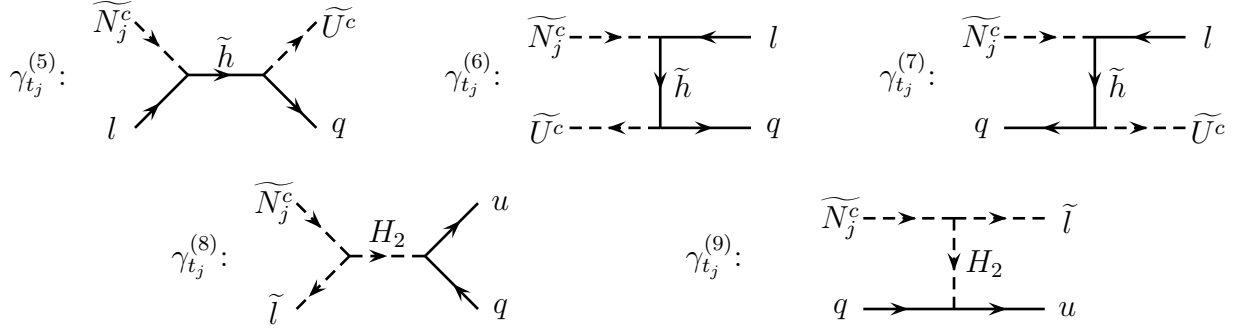


Figure 7: *Sneutrino-(s)top scattering.*

For the scalar neutrinos we have similarly (cf. fig. 7)

$$\begin{aligned}
\gamma_{t_j}^{(5)} &= \gamma(\widetilde{N}_j^c + l \leftrightarrow q + \widetilde{U}^c) = \gamma(\widetilde{N}_j^c + l \leftrightarrow \widetilde{q} + \widetilde{u}) , \\
\gamma_{t_j}^{(6)} &= \gamma(\widetilde{N}_j^c + \widetilde{U}^{c\dagger} \leftrightarrow \bar{l} + q) = \gamma(\widetilde{N}_j^c + \widetilde{q}^\dagger \leftrightarrow \bar{l} + \bar{u}) , \\
\gamma_{t_j}^{(7)} &= \gamma(\widetilde{N}_j^c + \bar{q} \leftrightarrow \bar{l} + \widetilde{U}^c) = \gamma(\widetilde{N}_j^c + u \leftrightarrow \bar{l} + \widetilde{q}) , \\
\gamma_{t_j}^{(8)} &= \gamma(\widetilde{N}_j^c + \bar{l}^\dagger \leftrightarrow \bar{q} + u) , \\
\gamma_{t_j}^{(9)} &= \gamma(\widetilde{N}_j^c + q \leftrightarrow \bar{l} + u) = \gamma(\widetilde{N}_j^c + \bar{u} \leftrightarrow \bar{l} + \bar{q}) .
\end{aligned}$$

The quartic scalar couplings of the sneutrinos give additional $2 \rightarrow 3$, $3 \rightarrow 3$ and $2 \rightarrow 4$ processes, which can be neglected since they are phase space suppressed.

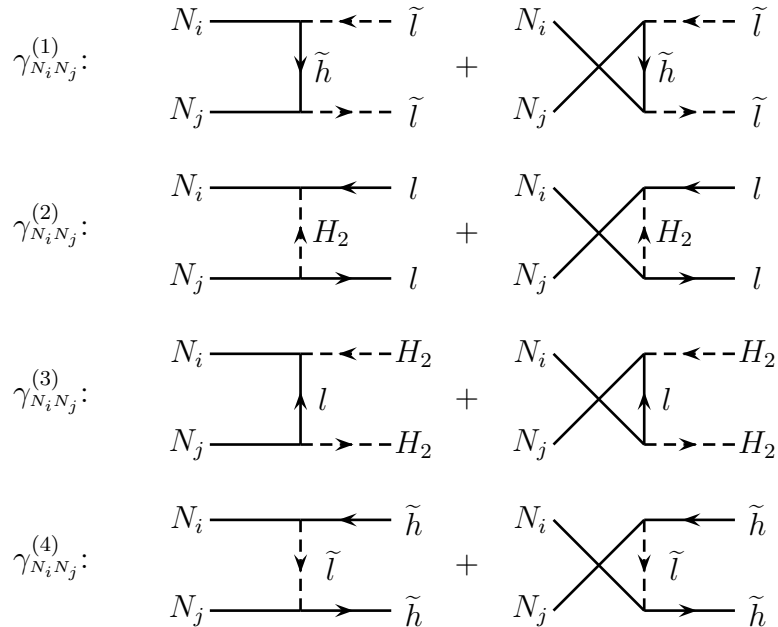


Figure 8: *Neutrino pair annihilation.*

2.5 Neutrino pair creation and annihilation

The Yukawa couplings of the right-handed neutrinos also allow lepton number conserving processes like the neutrino pair creation and annihilation.

For the neutrinos we have the processes depicted in fig. 8,

$$\begin{aligned}\gamma_{N_i N_j}^{(1)} &= \gamma(N_i + N_j \leftrightarrow \tilde{l} + \tilde{l}^\dagger), & \gamma_{N_i N_j}^{(2)} &= \gamma(N_i + N_j \leftrightarrow l + \bar{l}), \\ \gamma_{N_i N_j}^{(3)} &= \gamma(N_i + N_j \leftrightarrow H_2 + H_2^\dagger), & \gamma_{N_i N_j}^{(4)} &= \gamma(N_i + N_j \leftrightarrow \tilde{h} + \bar{\tilde{h}}).\end{aligned}$$

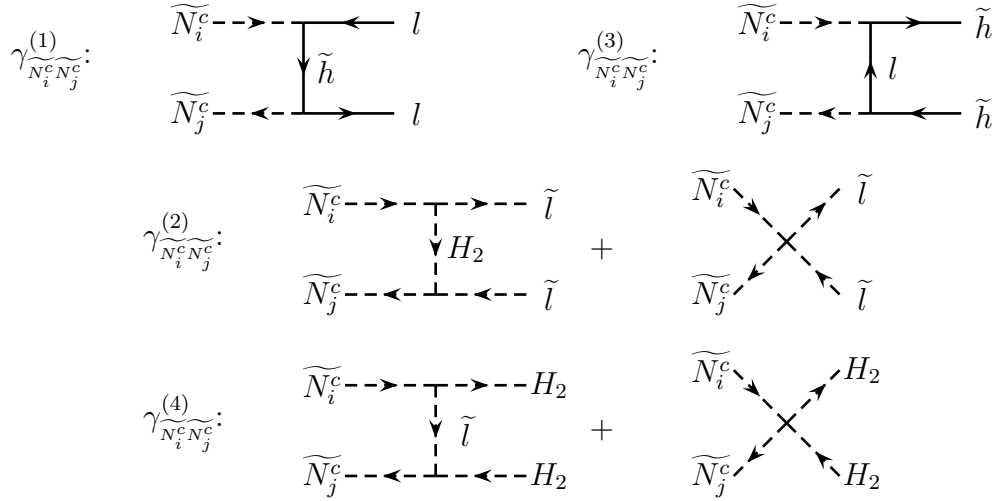


Figure 9: *Sneutrino pair annihilation.*

For the scalar neutrinos we have similar diagrams and additional contributions from the scalar potential (cf. fig. 9). We have the following reaction densities

$$\begin{aligned}\gamma_{\widetilde{N}_i^c \widetilde{N}_j^c}^{(1)} &= \gamma(\widetilde{N}_i^c + \widetilde{N}_j^{c\dagger} \leftrightarrow l + \bar{l}), & \gamma_{\widetilde{N}_i^c \widetilde{N}_j^c}^{(2)} &= \gamma(\widetilde{N}_i^c + \widetilde{N}_j^{c\dagger} \leftrightarrow \tilde{l} + \tilde{l}^\dagger), \\ \gamma_{\widetilde{N}_i^c \widetilde{N}_j^c}^{(3)} &= \gamma(\widetilde{N}_i^c + \widetilde{N}_j^{c\dagger} \leftrightarrow \tilde{h} + \bar{\tilde{h}}), & \gamma_{\widetilde{N}_i^c \widetilde{N}_j^c}^{(4)} &= \gamma(\widetilde{N}_i^c + \widetilde{N}_j^{c\dagger} \leftrightarrow H_2 + H_2^\dagger).\end{aligned}$$

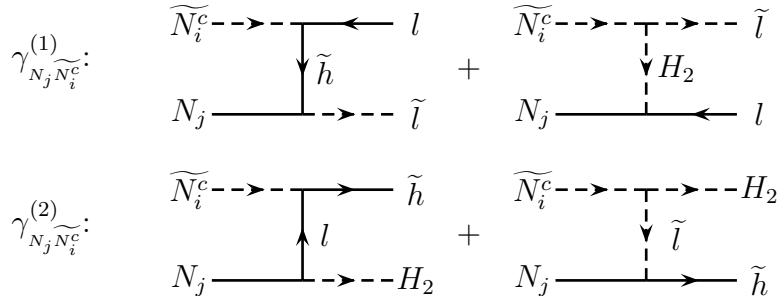


Figure 10: *Neutrino-sneutrino scattering.*



Figure 11: *Example of a L_f and L_s violating MSSM process.*

Finally, there are neutrino-sneutrino scattering processes (cf. fig. 10),

$$\gamma_{N_j \widetilde{N}_i^c}^{(1)} = \gamma(\widetilde{N}_i^c + N_j \leftrightarrow \bar{l} + \tilde{l}) , \quad \gamma_{N_j \widetilde{N}_i^c}^{(2)} = \gamma(\widetilde{N}_i^c + N_j \leftrightarrow \tilde{h} + H_2) .$$

Such diagrams also give neutrino-sneutrino transitions like $\widetilde{N}_i^c + l \leftrightarrow N_j + \tilde{l}$. These processes transform neutrinos into sneutrinos and leptons into sleptons, i.e. they tend to balance out the number densities of the fermions and their supersymmetric partners, but they cannot wash out any generated asymmetry. As we will see in the next chapter, the number densities of the neutrinos and the scalar neutrinos are already equal without taking into account these interactions, while the equality of the number densities of leptons and sleptons is ensured by MSSM-processes (cf. section 2.6). Finally, the dominant contributions to these neutrino-sneutrino transitions come from inverse decays, decays and scatterings off a (s)top which we have already considered. Hence, we can neglect these additional processes.

2.6 MSSM processes

In the MSSM the fermionic lepton number L_f and the lepton number stored in the scalar leptons L_s are not separately conserved. There are processes transforming leptons into scalar leptons and vice versa. As an example we have considered the process $e + e \leftrightarrow \tilde{e} + \tilde{e}$ (cf. fig. 11). For large temperatures, i.e. $s \gg m_\gamma^2$, the reduced cross section for this process is given by [15]

$$\hat{\sigma}_{\text{MSSM}} \approx 4\pi\alpha^2 \left[\ln \left(\frac{s}{m_\gamma^2} \right) - 4 \right] . \quad (16)$$

This translates into the following reaction density

$$\gamma_{\text{MSSM}} \approx \frac{M_1^4 \alpha^2}{4\pi^3} \frac{1}{z^4} \left[\ln \left(\frac{4}{z^2 a_\gamma} \right) - 2\gamma_E - 3 \right] , \quad (17)$$

where we have introduced the dimensionless squared photino mass

$$a_\gamma := \left(\frac{m_\gamma}{M_1} \right)^2 . \quad (18)$$

These processes are in thermal equilibrium if the reaction rates are larger than the Hubble parameter H . This condition gives a very weak upper bound on the photino mass,

$$m_\gamma \lesssim 2.5 \times 10^9 \text{ GeV} \left(\frac{T}{10^{10} \text{ GeV}} \right) \exp \left[-\frac{1}{412} \left(\frac{T}{10^{10} \text{ GeV}} \right) \right] . \quad (19)$$

In the calculations we assume $m_\gamma = 100 \text{ GeV}$.

3 Results

3.1 The Boltzmann equations

Now that we have identified all the relevant processes we can write down the network of Boltzmann equations which governs the time evolution of the neutrino and sneutrino number densities and of the lepton asymmetry. For the scalar neutrinos and their antiparticles it is convenient to use the sum and the difference of the particle numbers per comoving volume element as independent variables,

$$Y_{j\pm} := Y_{\widetilde{N}_j^c} \pm Y_{\widetilde{N}_j^{\dagger c}}. \quad (20)$$

Furthermore, we have to discern the lepton asymmetry stored in the Standard Model particles Y_{L_f} and the asymmetry Y_{L_s} in the scalar leptons.

For the neutrinos N_j one has

$$\begin{aligned} \frac{dY_{N_j}}{dz} = \frac{-z}{sH(M_1)} & \left\{ \left(\frac{Y_{N_j}}{Y_{N_j}^{\text{eq}}} - 1 \right) \left[\gamma_{N_j} + 4\gamma_{t_j}^{(0)} + 4\gamma_{t_j}^{(1)} + 4\gamma_{t_j}^{(2)} + 2\gamma_{t_j}^{(3)} + 4\gamma_{t_j}^{(4)} \right] \right. \\ & \left. + \sum_i \left[\left(\frac{Y_{N_j} Y_{N_i}}{Y_{N_j}^{\text{eq}} Y_{N_i}^{\text{eq}}} - 1 \right) \sum_{k=1}^4 \gamma_{N_i N_j}^{(k)} + \left(\frac{Y_{N_j} Y_{i_+}}{Y_{N_j}^{\text{eq}} Y_{N_i^c}^{\text{eq}}} - 2 \right) \sum_{k=1}^2 \gamma_{N_j \widetilde{N}_i^c}^{(k)} \right] \right\}. \end{aligned} \quad (21)$$

Correspondingly the Boltzmann equations for the scalar neutrinos read

$$\begin{aligned} \frac{dY_{j_+}}{dz} = \frac{-z}{sH(M_1)} & \left\{ \left(\frac{Y_{j_+}}{Y_{N_j^c}^{\text{eq}}} - 2 \right) \left(\gamma_{N_j^c}^{(2)} + \gamma_{N_j^c}^{(3)} + 3\gamma_{22_j} + 2\gamma_{t_j}^{(5)} + 2\gamma_{t_j}^{(6)} + 2\gamma_{t_j}^{(7)} + \gamma_{t_j}^{(8)} + 2\gamma_{t_j}^{(9)} \right) \right. \\ & + \frac{1}{2} \frac{Y_{j_-} Y_{L_s}}{Y_{N_j^c}^{\text{eq}} Y_l^{\text{eq}}} \left(\gamma_{22_j} - \gamma_{t_j}^{(8)} \right) + \frac{Y_{j_-} Y_{L_f}}{Y_{N_j^c}^{\text{eq}} Y_l^{\text{eq}}} \gamma_{t_j}^{(5)} \\ & \left. + \sum_i \left[\frac{1}{2} \left(\frac{Y_{j_+} Y_{i_+}}{Y_{N_j^c}^{\text{eq}} Y_{N_i^c}^{\text{eq}}} - \frac{Y_{j_-} Y_{i_-}}{Y_{N_j^c}^{\text{eq}} Y_{N_i^c}^{\text{eq}}} - 4 \right) \sum_{k=1}^4 \gamma_{N_i^c N_j^c}^{(k)} + \left(\frac{Y_{j_+} Y_{N_i}}{Y_{N_j^c}^{\text{eq}} Y_{N_i}^{\text{eq}}} - 2 \right) \sum_{k=1}^2 \gamma_{N_i^c \widetilde{N}_j^c}^{(k)} \right] \right\}, \end{aligned} \quad (22)$$

$$\begin{aligned} \frac{dY_{j_-}}{dz} = \frac{-z}{sH(M_1)} & \left\{ \frac{Y_{j_-}}{Y_{N_j^c}^{\text{eq}}} \left(\gamma_{N_j^c}^{(2)} + \gamma_{N_j^c}^{(3)} + 3\gamma_{22_j} + 2\gamma_{t_j}^{(5)} + 2\gamma_{t_j}^{(6)} + 2\gamma_{t_j}^{(7)} + \gamma_{t_j}^{(8)} + 2\gamma_{t_j}^{(9)} \right) \right. \\ & + \frac{Y_{L_s}}{Y_l^{\text{eq}}} \left[\gamma_{N_j^c}^{(3)} - \frac{1}{2} \gamma_{N_j^c}^{(2)} - 2\gamma_{t_j}^{(9)} - \frac{1}{2} \frac{Y_{j_+}}{Y_{N_j^c}^{\text{eq}}} \gamma_{t_j}^{(8)} + \left(2 + \frac{1}{2} \frac{Y_{j_+}}{Y_{N_j^c}^{\text{eq}}} \right) \gamma_{22_j} \right] \\ & \left. + \frac{Y_{L_f}}{Y_l^{\text{eq}}} \left[\frac{1}{2} \gamma_{N_j^c}^{(2)} + 2 \left(\gamma_{t_j}^{(6)} + \gamma_{t_j}^{(7)} \right) + \frac{Y_{j_+}}{Y_{N_j^c}^{\text{eq}}} \gamma_{t_j}^{(5)} \right] \right\} \end{aligned} \quad (23)$$

$$+ \sum_i \left[\frac{1}{2} \left(\frac{Y_{j-} Y_{i+}}{\widetilde{Y}_{N_j^c}^{\text{eq}} \widetilde{Y}_{N_i^c}^{\text{eq}}} - \frac{Y_{j+} Y_{i-}}{\widetilde{Y}_{N_j^c}^{\text{eq}} \widetilde{Y}_{N_i^c}^{\text{eq}}} \right) \sum_{k=1}^4 \widetilde{\gamma}_{N_i^c N_j^c}^{(k)} + \frac{Y_{j-} Y_{N_i}}{\widetilde{Y}_{N_j^c}^{\text{eq}} \widetilde{Y}_{N_i}^{\text{eq}}} \sum_{k=1}^2 \widetilde{\gamma}_{N_i^c N_j^c}^{(k)} + \left(\frac{Y_{L_f}}{\widetilde{Y}_l^{\text{eq}}} - \frac{Y_{L_s}}{\widetilde{Y}_l^{\text{eq}}} \right) \widetilde{\gamma}_{N_i^c N_j^c}^{(1)} \right] \Bigg\} .$$

The Boltzmann equations for the lepton asymmetries are given by

$$\begin{aligned} \frac{dY_{L_f}}{dz} = & \frac{-z}{sH(M_1)} \left\{ \sum_j \left[\left(\frac{1}{2} \frac{Y_{L_f}}{\widetilde{Y}_l^{\text{eq}}} + \varepsilon_j \right) \left(\frac{1}{2} \gamma_{N_j} + \widetilde{\gamma}_{N_j^c}^{(2)} \right) - \frac{1}{2} \varepsilon_j \left(\frac{Y_{N_j}}{\widetilde{Y}_{N_j}^{\text{eq}}} \gamma_{N_j} + \frac{Y_{j+}}{\widetilde{Y}_{N_j^c}^{\text{eq}}} \widetilde{\gamma}_{N_j^c}^{(2)} \right) + \frac{1}{2} \frac{Y_{j-}}{\widetilde{Y}_{N_j^c}^{\text{eq}}} \widetilde{\gamma}_{N_j^c}^{(2)} \right] \right. \\ & + \frac{Y_{L_f}}{\widetilde{Y}_l^{\text{eq}}} (\gamma_A^{\Delta L} + \gamma_C^{\Delta L}) + \frac{Y_{L_s}}{\widetilde{Y}_l^{\text{eq}}} (\gamma_B^{\Delta L} - \gamma_C^{\Delta L}) + \left(\frac{Y_{L_f}}{\widetilde{Y}_l^{\text{eq}}} - \frac{Y_{L_s}}{\widetilde{Y}_l^{\text{eq}}} \right) \gamma_{\text{MSSM}} \\ & + \sum_j \left[\frac{Y_{L_f}}{\widetilde{Y}_l^{\text{eq}}} \left(\frac{Y_{N_j}}{\widetilde{Y}_{N_j}^{\text{eq}}} \gamma_{t_j}^{(3)} + \frac{Y_{j+}}{\widetilde{Y}_{N_j^c}^{\text{eq}}} \gamma_{t_j}^{(5)} + 2\gamma_{t_j}^{(4)} + 2\gamma_{t_j}^{(6)} + 2\gamma_{t_j}^{(7)} \right) + 2 \frac{Y_{j-}}{\widetilde{Y}_{N_j^c}^{\text{eq}}} (\gamma_{t_j}^{(5)} + \gamma_{t_j}^{(6)} + \gamma_{t_j}^{(7)}) \right] \\ & \left. + \sum_{i,j} \left(\frac{Y_{L_f}}{\widetilde{Y}_l^{\text{eq}}} - \frac{Y_{L_s}}{\widetilde{Y}_l^{\text{eq}}} + \frac{Y_{N_j}}{\widetilde{Y}_{N_j}^{\text{eq}}} \frac{Y_{i-}}{\widetilde{Y}_{N_i^c}^{\text{eq}}} \right) \widetilde{\gamma}_{N_j^c N_i^c}^{(1)} \right\} , \end{aligned} \quad (24)$$

$$\begin{aligned} \frac{dY_{L_s}}{dz} = & \frac{-z}{sH(M_1)} \left\{ \sum_j \left[\left(\frac{1}{2} \frac{Y_{L_s}}{\widetilde{Y}_l^{\text{eq}}} + \varepsilon_j \right) \left(\frac{1}{2} \gamma_{N_j} + \widetilde{\gamma}_{N_j^c}^{(2)} \right) - \frac{1}{2} \varepsilon_j \left(\frac{Y_{N_j}}{\widetilde{Y}_{N_j}^{\text{eq}}} \gamma_{N_j} + \frac{Y_{j+}}{\widetilde{Y}_{N_j^c}^{\text{eq}}} \widetilde{\gamma}_{N_j^c}^{(2)} \right) \right. \right. \\ & \left. - \frac{1}{2} \frac{Y_{j-}}{\widetilde{Y}_{N_j^c}^{\text{eq}}} \widetilde{\gamma}_{N_j^c}^{(2)} + \left(\frac{Y_{L_s}}{\widetilde{Y}_l^{\text{eq}}} + \frac{Y_{j-}}{\widetilde{Y}_{N_j^c}^{\text{eq}}} \right) \gamma_{N_j}^{(3)} + \left(\frac{1}{2} \frac{Y_{j+}}{\widetilde{Y}_{N_j^c}^{\text{eq}}} \frac{Y_{L_s}}{\widetilde{Y}_l^{\text{eq}}} + 2 \frac{Y_{L_s}}{\widetilde{Y}_l^{\text{eq}}} + 3 \frac{Y_{j-}}{\widetilde{Y}_{N_j^c}^{\text{eq}}} \right) \gamma_{22j} \right] \\ & + \frac{Y_{L_s}}{\widetilde{Y}_l^{\text{eq}}} (\gamma_A^{\Delta L} + \gamma_D^{\Delta L}) + \frac{Y_{L_f}}{\widetilde{Y}_l^{\text{eq}}} (\gamma_B^{\Delta L} - \gamma_C^{\Delta L}) + \left(\frac{Y_{L_s}}{\widetilde{Y}_l^{\text{eq}}} - \frac{Y_{L_f}}{\widetilde{Y}_l^{\text{eq}}} \right) \gamma_{\text{MSSM}} \\ & + \sum_j \left[\frac{Y_{L_s}}{\widetilde{Y}_l^{\text{eq}}} \left(2 \frac{Y_{N_j}}{\widetilde{Y}_{N_j}^{\text{eq}}} \gamma_{t_j}^{(0)} + \frac{1}{2} \frac{Y_{j+}}{\widetilde{Y}_{N_j^c}^{\text{eq}}} \gamma_{t_j}^{(8)} + 2\gamma_{t_j}^{(1)} + 2\gamma_{t_j}^{(2)} + 2\gamma_{t_j}^{(9)} \right) - \frac{Y_{j-}}{\widetilde{Y}_{N_j^c}^{\text{eq}}} (\gamma_{t_j}^{(8)} + 2\gamma_{t_j}^{(9)}) \right] \\ & \left. + \sum_{i,j} \left(\frac{Y_{L_s}}{\widetilde{Y}_l^{\text{eq}}} - \frac{Y_{L_f}}{\widetilde{Y}_l^{\text{eq}}} - \frac{Y_{N_j}}{\widetilde{Y}_{N_j}^{\text{eq}}} \frac{Y_{i-}}{\widetilde{Y}_{N_i^c}^{\text{eq}}} \right) \widetilde{\gamma}_{N_j^c N_i^c}^{(1)} \right\} , \end{aligned} \quad (25)$$

where we have introduced the following abbreviations for the lepton number violating scatterings mediated by a heavy (s)neutrino

$$\gamma_A^{\Delta L} = 2\gamma_N^{(1)} + \gamma_N^{(3)} + \gamma_N^{(4)} + \gamma_N^{(6)} + \gamma_N^{(7)} + 2\gamma_N^{(12)} + \gamma_N^{(14)} , \quad (26)$$

$$\gamma_B^{\Delta L} = \gamma_N^{(3)} + \gamma_N^{(4)} - \gamma_N^{(6)} - \gamma_N^{(7)} + \gamma_N^{(14)} , \quad (27)$$

$$\gamma_C^{\Delta L} = 3\gamma_N^{(9)} + \gamma_N^{(17)} + \gamma_N^{(18)} + 6\gamma_N^{(19)} , \quad (28)$$

$$\gamma_D^{\Delta L} = 4\gamma_N^{(5)} + 2\gamma_N^{(8)} + 8\gamma_N^{(10)} + 3\gamma_N^{(9)} + 4\gamma_N^{(15)} + 2\gamma_N^{(16)} + \gamma_N^{(17)} + \gamma_N^{(18)} + 6\gamma_N^{(19)} . \quad (29)$$

The numerical factors in front of the reaction densities arise due to the change in quantum numbers in the corresponding scattering, e.g. processes transforming leptons into sleptons appear with a relative minus sign in the Boltzmann equations for Y_{L_f} and Y_{L_s} . Furthermore, any reaction density is multiplied by the number of different processes (cf. section 2) contributing independently to the Boltzmann equations.

This set of Boltzmann equations is valid for the most general case with arbitrary masses of the right-handed neutrinos. However, if the heavy neutrinos are mass degenerate, it is always possible to find a basis where the mass matrix M and the Yukawa matrix λ_ν are diagonal, i.e. no asymmetry is generated. Therefore, one has to assume a mass hierarchy for the right-handed neutrinos, which in turn implies that the lepton number violating processes induced by the lightest right-handed neutrino are in thermal equilibrium as long as the temperature is higher than the mass of this neutrino. Hence, the lepton asymmetries generated in the decays of the heavier right-handed neutrinos are washed out and the asymmetry that we observe today must have been generated by the lightest right-handed neutrino. We will assume that the first generation neutrino N_1 is the lightest.

Hence, in the following we will always neglect the heavier right-handed neutrinos as free particles. However, they have to be taken into account as intermediate states since they give a substantial contribution to the effective lepton number violating processes at low energies.

The fermionic part Y_{L_f} of the generated lepton asymmetry will be transformed into a $(B-L)$ asymmetry by the action of sphalerons. But since MSSM processes like the one in section 2.6 enforce the relation

$$Y_{L_f} = Y_{L_s} , \quad (30)$$

the total lepton asymmetry $Y_L = Y_{L_f} + Y_{L_s}$ will be proportional to the baryon asymmetry [16],

$$Y_B = - \left(\frac{8N_f + 4N_H}{22N_f + 13N_H} \right) Y_L , \quad (31)$$

where N_f is the number of quark-lepton families and N_H is the number of Higgs doublets. In our model with $N_f = 3$ and $N_H = 2$ we have

$$Y_B = -\frac{8}{23} Y_L . \quad (32)$$

From eqs. (1) and (30) we can infer the asymmetries that we have to generate,

$$Y_{L_f} = Y_{L_s} = -(0.9 - 1.4) \cdot 10^{-10} . \quad (33)$$

The additional anomalous global symmetries in supersymmetric theories at high temperatures have no influence on these considerations, since they are broken well before the electroweak phase transition [17].

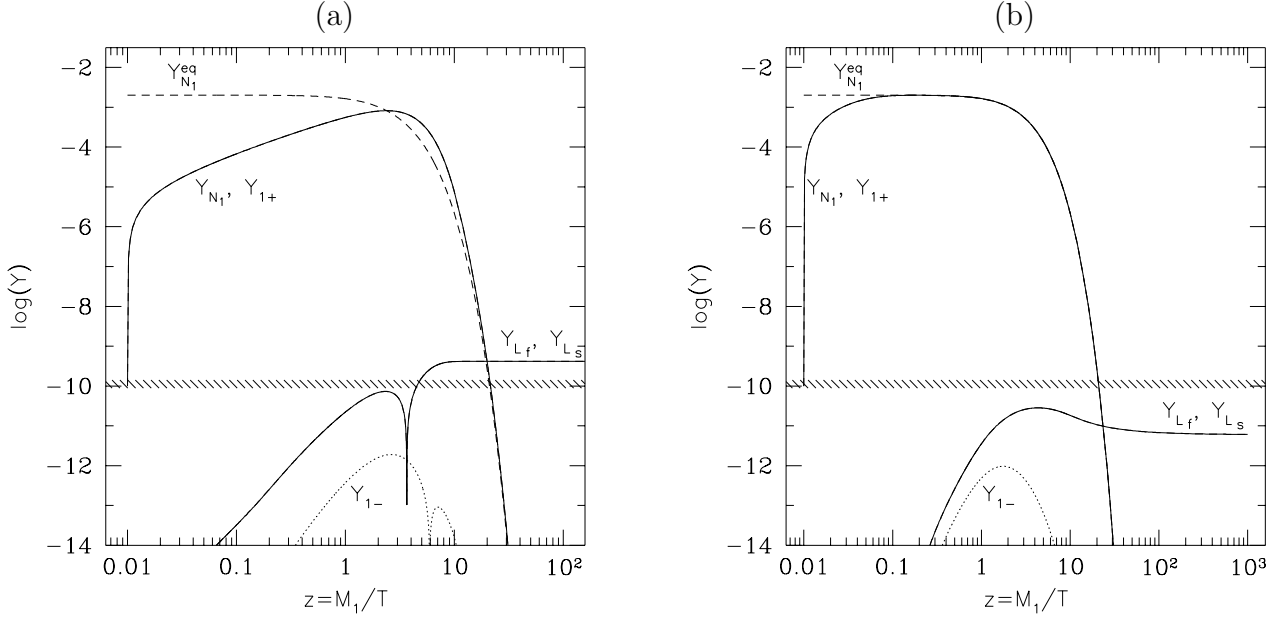


Figure 12: *Typical solutions of the Boltzmann equations. The dashed line represents the equilibrium distribution for the neutrinos N_1 and the solid lines show the solutions for the (s)neutrino number and the absolute values of the asymmetries in L_f and L_s , while the dotted line represents the absolute value of the scalar neutrino asymmetry Y_{1-} . The lines for Y_{N_1} and Y_{1+} and for the two asymmetries Y_{L_f} and Y_{L_s} cannot be distinguished, since they are lying one upon another. The hatched area shows the measured value (33).*

3.2 The generated lepton asymmetry

Typical solutions of the Boltzmann equations are shown in fig. 12, where we have assumed a neutrino mass $M_1 = 10^{10}$ GeV and a mass hierarchy of the form

$$a_2 = 10^3, \quad (m_D^\dagger m_D)_{22} = a_2 (m_D^\dagger m_D)_{11}, \quad (34)$$

$$a_3 = 10^6, \quad (m_D^\dagger m_D)_{33} = a_3 (m_D^\dagger m_D)_{11}. \quad (35)$$

Furthermore we have assumed a CP asymmetry $\varepsilon_1 = -10^{-6}$. The only difference between both figures lies in the choice of $(m_D^\dagger m_D)_{11}$:

$$\tilde{m}_1 := \frac{(m_D^\dagger m_D)_{11}}{M_1} = \begin{cases} 10^{-4} \text{ eV} & \text{for fig. 12a,} \\ 10^{-2} \text{ eV} & \text{for fig. 12b.} \end{cases} \quad (36)$$

Finally, as starting condition we have assumed that all the number densities vanish at high temperatures $T \gg M_1$, including the neutrino numbers Y_{N_1} and Y_{1+} . As one can see, the Yukawa interactions are strong enough to create a substantial number of neutrinos and scalar neutrinos in fig. 12a, even if Y_{N_1} and Y_{1+} do not reach their equilibrium values as long as $z < 1$. However, the generated asymmetries

$$Y_{L_f} = Y_{L_s} = -4 \cdot 10^{-10} \quad (37)$$

are of the requested magnitude. On the other hand, in fig. 12b the Yukawa interactions are much stronger, i.e. the neutrinos are driven into equilibrium rapidly at high temperatures. However, the large Yukawa couplings also increase the reaction rates for the lepton number violating processes which can wash out a generated asymmetry, i.e. the final asymmetries are much smaller than in the previous case,

$$Y_{L_f} = Y_{L_s} = -6 \cdot 10^{-12}. \quad (38)$$

In both cases a small scalar neutrino asymmetry Y_{1-} is temporarily generated. However, Y_{1-} is very small and has virtually no influence on the generated lepton asymmetries.

Usually it is assumed that one has a thermal population of right-handed neutrinos at high temperatures which decay at very low temperatures $T \ll M_1$ where one can neglect lepton number violating scatterings. Then the generated lepton asymmetry is proportional to the CP asymmetry and the number of decaying neutrinos and sneutrinos [1],

$$Y_L \approx \varepsilon_1 \left[Y_{N_1}^{\text{eq}}(T \gg M_1) + Y_{1+}^{\text{eq}}(T \gg M_1) \right] \approx \frac{\varepsilon_1}{250}. \quad (39)$$

With $\varepsilon_1 = -10^{-6}$ this gives

$$Y_{L_f} = Y_{L_s} \approx -2 \cdot 10^{-9}. \quad (40)$$

By comparison with eqs. (37) and (38) one sees that by assuming a thermal population of heavy neutrinos at high temperatures and neglecting the lepton number violating scatterings one largely overestimates the generated lepton asymmetries.

A characteristic feature of the non-supersymmetric version of this baryogenesis mechanism is that the generated asymmetry does not depend on the neutrino mass M_1 and $(m_D^\dagger m_D)_{11}$ separately but only on the ratio \widetilde{m}_1 [11]. To check if this is also the case in the supersymmetric scenario we have varied \widetilde{m}_1 while keeping all the other parameters fixed. In fig. 13 we have plotted the total lepton asymmetry $Y_L = Y_{L_f} + Y_{L_s}$ as a function of \widetilde{m}_1 for the right-handed neutrino masses $M_1 = 10^{12}$ GeV, 10^{10} GeV and 10^8 GeV, and the CP asymmetry $\varepsilon_1 = -10^{-6}$.

The main difference between the supersymmetric and non-supersymmetric scenarios concerns the necessary production of the neutrinos at high temperatures. In the non-supersymmetric scenario the Yukawa interactions are too weak to account for this, i.e. additional interactions of the right-handed neutrinos have to be introduced. This is no longer the case here. The supersymmetric Yukawa interactions are much more important, and can produce a thermal population of right-handed neutrinos, i.e. the same vertices which are responsible for the generation of the asymmetry can also bring the neutrinos into thermal equilibrium at high temperatures. However, these lepton number violating processes will also erase a part of the generated asymmetry, hereby giving rise to the \widetilde{m}_1 dependence of the generated asymmetry which we shall discuss in detail.

First one sees that in the whole parameter range the generated asymmetry is much smaller than the naively expected value $4 \cdot 10^{-9}$. For low \widetilde{m}_1 the reason being that the Yukawa interactions are too weak to bring the neutrinos into equilibrium at high temperatures, like in

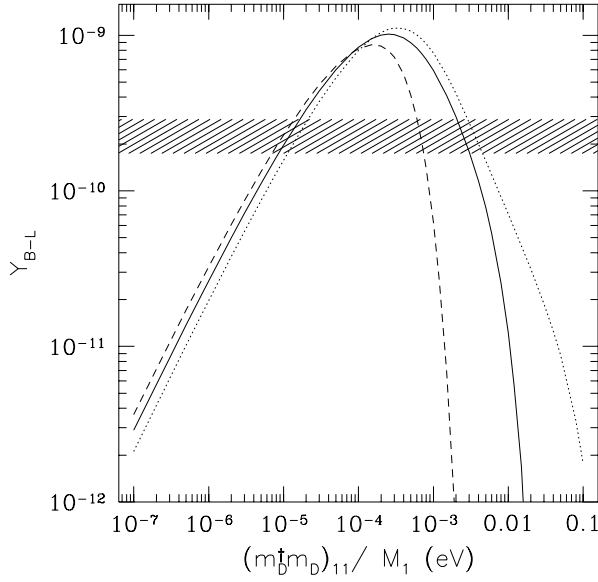


Figure 13: *Generated (B – L) asymmetry as a function of \tilde{m}_1 for $M_1 = 10^8$ GeV (dotted line), $M_1 = 10^{10}$ GeV (solid line) and $M_1 = 10^{12}$ GeV (dashed line). The shaded area shows the measured value for the asymmetry.*

fig. 12a. For high \tilde{m}_1 on the other hand, the lepton number violating scatterings wash out a large part of the generated asymmetry at temperatures $T < M_1$, like in fig. 12b. Hence, the requested asymmetry can only be generated if \tilde{m}_1 is larger than $\sim 10^{-5}$ eV and smaller than $\sim 5 \cdot 10^{-3}$ eV, depending on the heavy neutrino mass M_1 .

The asymmetry in fig. 13 depends almost only on \tilde{m}_1 for small $\tilde{m}_1 \lesssim 10^{-4}$ eV, since in this region of parameter space the asymmetry depends mostly on the number of neutrinos generated at high temperatures, i.e. on the strength of the processes in which a right-handed neutrino can be generated or annihilated. The dominant reactions are decays, inverse decays and scatterings with a (s)top, which all give contributions proportional to \tilde{m}_1 to the Boltzmann equations at high temperatures,

$$\begin{aligned}
 \frac{-z}{sH(M_1)} \gamma_{N_1} &\propto \tilde{m}_1, & \frac{-z}{sH(M_1)} \gamma_{N_1^c}^{(2)} &\propto \tilde{m}_1, & \frac{-z}{sH(M_1)} \gamma_{N_1^c}^{(3)} &\propto \tilde{m}_1, \\
 \frac{-z}{sH(M_1)} \gamma_{22_1} &\propto \tilde{m}_1, & \frac{-z}{sH(M_1)} \gamma_{t_1}^{(i)} (T \gg M_1) &\propto \tilde{m}_1. & &
 \end{aligned} \tag{41}$$

For large $\tilde{m}_1 \gtrsim 10^{-4}$ eV on the other hand, the neutrinos reach thermal equilibrium at high temperatures, i.e. the generated asymmetry depends mostly on the influence of the lepton number violating scatterings at temperatures $T \lesssim M_1$. In contrast to the relations of eq. (41) the lepton number violating processes mediated by a heavy neutrino behave like

$$\frac{-z}{sH(M_1)} \gamma_i^{\Delta L} \propto M_1 \sum_j \tilde{m}_j^2, \quad i = A, \dots, D \tag{42}$$

at low temperatures. Hence, one expects that the generated asymmetry becomes smaller for growing neutrino mass M_1 and this is exactly what one observes in fig. 13.

The lepton number violating scatterings can also explain the small dependence of the asymmetry on the heavy neutrino mass M_1 for $\widetilde{m}_1 \lesssim 10^{-4}$ eV. The inverse decay processes which take part in producing the neutrinos at high temperatures are CP violating, i.e. they generate a lepton asymmetry at high temperatures. Due to the interplay of inverse decay processes and lepton number violating $2 \rightarrow 2$ scatterings this asymmetry has a different sign compared to the one generated in neutrino decays at low temperatures, i.e. the asymmetries will partially cancel each other, as one can see in the change of sign of the asymmetry in fig. 12a. This cancellation can only be avoided if the asymmetry generated at high temperatures is washed out before the neutrinos decay. At high temperatures the lepton number violating scatterings behave like

$$\frac{-z}{sH(M_1)} \gamma_i^{\Delta L} \propto M_1 \sum_j a_j \widetilde{m}_j^2, \quad i = A, \dots, D. \quad (43)$$

Hence, the wash-out processes are more efficient for larger neutrino masses, i.e. the final asymmetry should grow with the neutrino mass M_1 . The finally generated asymmetry is not affected by the stronger wash-out processes, since for small \widetilde{m}_1 the neutrinos decay late, where one can neglect the lepton number violating scatterings.

This change of sign in the asymmetry is not observed in fig. 12b. Due to the larger \widetilde{m}_1 value the neutrinos are brought into equilibrium at much higher temperatures, where decays and inverse decays are suppressed by a time dilatation factor, i.e. the (s)neutrinos are produced in CP invariant scatterings off a (s)top.

4 SO(10) unification and leptogenesis

In ref. [12], it was shown that there is no direct connection between CP violation and leptonic flavour mixing at high and low energies. Furthermore, the implications of non-supersymmetric leptogenesis on the scale of $(B - L)$ breaking and the light neutrino masses have been studied by assuming a similar pattern of masses and mixings for the leptons and the quarks. Here we are going to repeat this analysis for the supersymmetric scenario.

4.1 Neutrino masses and mixings

If we choose a basis where the Majorana mass matrix M and the Dirac mass matrix m_l for the charged leptons are diagonal with real and positive eigenvalues,

$$m_l = \begin{pmatrix} m_e & 0 & 0 \\ 0 & m_\mu & 0 \\ 0 & 0 & m_\tau \end{pmatrix}, \quad M = \begin{pmatrix} M_1 & 0 & 0 \\ 0 & M_2 & 0 \\ 0 & 0 & M_3 \end{pmatrix}, \quad (44)$$

the Dirac mass matrix of the neutrinos can be written in the form

$$m_D = V \begin{pmatrix} m_1 & 0 & 0 \\ 0 & m_2 & 0 \\ 0 & 0 & m_3 \end{pmatrix} U^\dagger, \quad (45)$$

where V and U are unitary matrices and the m_i are real and positive.

All the quantities relevant for baryogenesis depend only on the product $m_D^\dagger m_D$, which is determined by the Dirac masses m_i and the three mixing angles and six phases of U . Five of these phases can be factored out with the Gell-Mann matrices λ_i ,

$$U = e^{i\gamma} e^{i\lambda_3\alpha} e^{i\lambda_8\beta} U_1 e^{i\lambda_3\sigma} e^{i\lambda_8\tau}. \quad (46)$$

In analogy to the Kobayashi-Maskawa matrix for quarks the remaining matrix U_1 depends on three mixing angles and one phase. In unified theories based on SO(10) it is natural to assume a similar pattern of masses and mixings for leptons and quarks. This suggests the Wolfenstein parametrization [18] as ansatz for U_1 ,

$$U_1 = \begin{pmatrix} 1 - \frac{\lambda^2}{2} & \lambda & A\lambda^3(\rho - i\eta) \\ -\lambda & 1 - \frac{\lambda^2}{2} & A\lambda^2 \\ A\lambda^3(1 - \rho - i\eta) & -A\lambda^2 & 1 \end{pmatrix}, \quad (47)$$

where A and $|\rho + i\eta|$ are of order one, while the mixing parameter λ is assumed to be small. For the Dirac masses m_i SO(10) unification motivates a hierarchy like for the up-type quarks,

$$m_1 = b\lambda^4 m_3 \quad m_2 = c\lambda^2 m_3 \quad b, c = \mathcal{O}(1). \quad (48)$$

We have mentioned in section 3.1 that we also need a hierarchy in the Majorana masses M_i to get a lepton asymmetry. We choose a similar hierarchy as in eq. (48),

$$M_1 = B\lambda^4 M_3 \quad M_2 = C\lambda^2 M_3 \quad B, C = \mathcal{O}(1). \quad (49)$$

Later on we will vary the parameters B and C to investigate different hierarchies for the right-handed neutrinos.

The light neutrino masses read [12]

$$m_{\nu_e} = \frac{b^2}{|C + e^{4i\alpha} B|} \lambda^4 m_{\nu_\tau} + \mathcal{O}(\lambda^6) \quad (50)$$

$$m_{\nu_\mu} = \frac{c^2 |C + e^{4i\alpha} B|}{BC} \lambda^2 m_{\nu_\tau} + \mathcal{O}(\lambda^4) \quad (51)$$

$$m_{\nu_\tau} = \frac{m_3^2}{M_3} + \mathcal{O}(\lambda^4). \quad (52)$$

We will not discuss the masses of the light scalar neutrinos here, since they depend on unknown soft breaking terms.

In section 3.2 we have seen that the lepton asymmetry is largely determined by the mass parameter \widetilde{m}_1 , which is given by

$$\widetilde{m}_1 = \frac{c^2 + A^2 |\rho + i\eta|^2}{B} \lambda^2 m_{\nu_\tau} , \quad (53)$$

i.e. \widetilde{m}_1 is of the same order as the ν_μ mass. From eq. (9) we get the CP asymmetry

$$\varepsilon_1 = \frac{3}{8\pi} \frac{B A^2}{c^2 + A^2 |\rho + i\eta|^2} \lambda^4 \frac{m_3^2}{v_2^2} \text{Im} [(\rho - i\eta)^2 e^{i2(\alpha + \sqrt{3}\beta)}] + \mathcal{O}(\lambda^6) . \quad (54)$$

In the next section we will always assume maximal phases, i.e. we will set

$$\varepsilon_1 = -\frac{3}{8\pi} \frac{B A^2 |\rho + i\eta|^2}{c^2 + A^2 |\rho + i\eta|^2} \lambda^4 \frac{m_3^2}{v_2^2} + \mathcal{O}(\lambda^6) . \quad (55)$$

Hence, the lepton asymmetries that we are going to calculate may be viewed as upper bounds on the attainable asymmetries.

Like in the non-supersymmetric scenario a large value of the Yukawa-coupling m_3/v_2 will be preferred by this baryogenesis mechanism, since $\varepsilon_1 \propto m_3^2/v_2^2$. This holds irrespective of our ansatz for neutrino mixings.

4.2 Numerical results

The neutrino masses (50)-(52) can be used to constrain the free parameters of our ansatz. The strongest hint for a non-vanishing neutrino mass being the solar neutrino deficit¹, we will fix the ν_μ mass to the value preferred by the MSW solution [19],

$$m_{\nu_\mu} \simeq 3 \cdot 10^{-3} \text{ eV} . \quad (56)$$

Hence the parameter \widetilde{m}_1 , which is of the same order as m_{ν_μ} according to eq. (53), will be in the interval allowed by fig. 13.

The most obvious parameter choice is to take all $\mathcal{O}(1)$ parameters equal to one and to fix λ to a similar value as the λ parameter of the quark mixing matrix,

$$A = B = C = b = c = |\rho + i\eta| \simeq 1 , \quad \lambda \simeq 0.1 . \quad (57)$$

The ν_μ mass in eqs. (51) and (56) then fixes the ν_e and ν_τ masses,

$$m_{\nu_e} \simeq 8 \cdot 10^{-6} \text{ eV} , \quad m_{\nu_\tau} \simeq 0.15 \text{ eV} \quad (58)$$

and \widetilde{m}_1 reads

$$\widetilde{m}_1 \simeq 3 \cdot 10^{-3} \text{ eV} . \quad (59)$$

SO(10) unification suggests that the Dirac neutrino mass m_3 is equal to the top-quark mass,

$$m_3 = m_t \simeq 174 \text{ GeV} . \quad (60)$$

¹For a review and references, see [20].

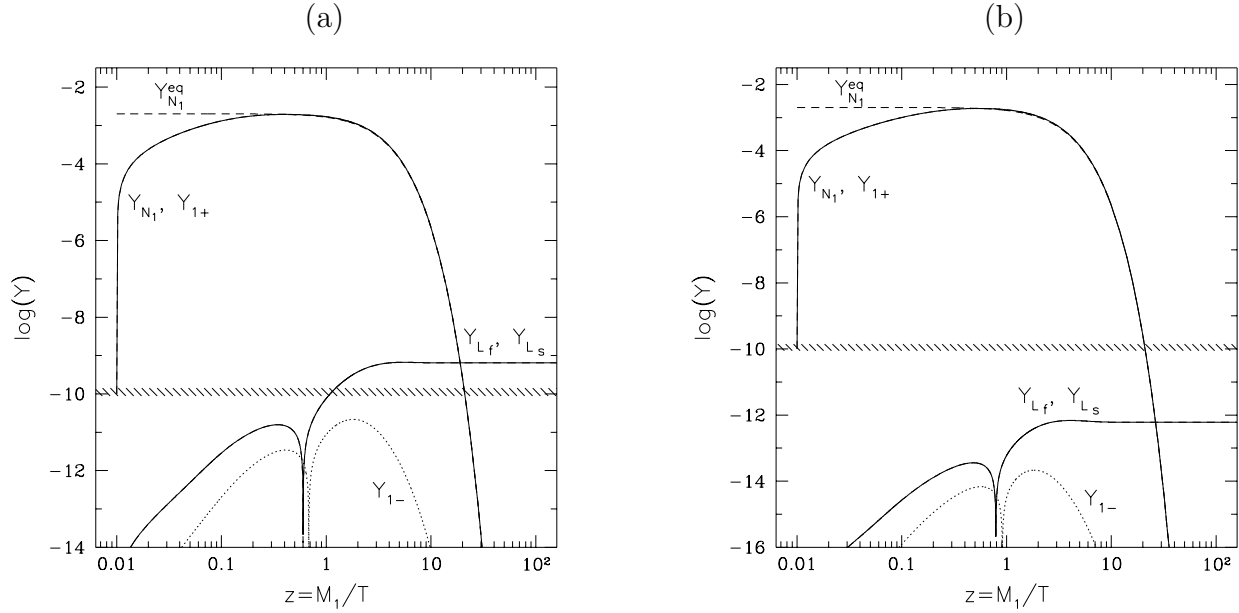


Figure 14: *Generated asymmetry if one assumes a similar pattern of masses and mixings for the leptons and the quarks. In both figures we have $\lambda = 0.1$ and $m_3 = m_t$ (a) and $m_3 = m_b$ (b).*

This leads to a large Majorana mass scale for the right-handed neutrinos,

$$M_3 \simeq 2 \cdot 10^{14} \text{ GeV} \quad \Rightarrow \quad M_1 \simeq 2 \cdot 10^{10} \text{ GeV} \text{ and } M_2 \simeq 2 \cdot 10^{12} \text{ GeV} , \quad (61)$$

and eq. (55) gives the CP asymmetry $\varepsilon_1 \simeq -6 \cdot 10^{-6}$. Integration of the Boltzmann equations yields the $(B - L)$ asymmetry (cf. fig. 14a)

$$Y_{B-L} \simeq 10^{-9} , \quad (62)$$

which is of the correct order of magnitude. It is interesting to note that in the non-supersymmetric scenario one has $Y_{B-L} \simeq 9 \cdot 10^{-10}$ for the same choice of parameters.

Our assumption (60), $m_3 \simeq m_t$ led to a large Majorana mass scale M_3 in eq. (61). To check the sensitivity of our result for the baryon asymmetry on this choice, we have envisaged a lower Dirac mass scale

$$m_3 = m_b \simeq 4.5 \text{ GeV} , \quad (63)$$

while keeping all other parameters in eq. (57) fixed. The assumed ν_μ mass (56) then requires a much lower value for the Majorana mass scale, $M_3 \simeq 10^{11} \text{ GeV}$ and the CP asymmetry $\varepsilon_1 \simeq -4 \cdot 10^{-9}$ becomes very small. Consequently, the generated asymmetry (cf. fig. 14b)

$$Y_{B-L} \simeq 10^{-12} , \quad (64)$$

is too small by more than two orders of magnitude. We can conclude that high values for both masses m_3 and M_3 are preferred. This suggests that $(B - L)$ is already broken at the unification

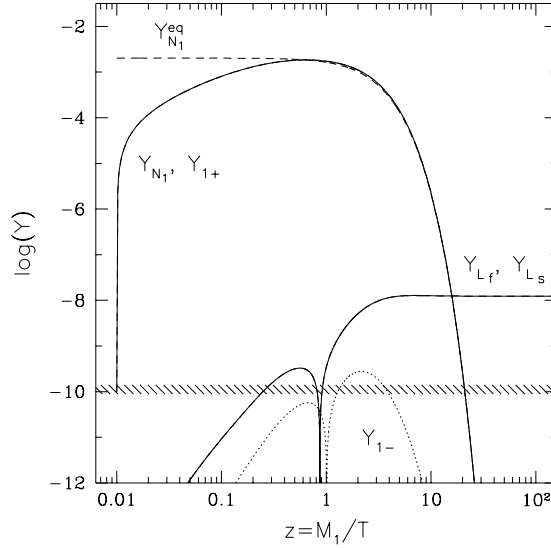


Figure 15: *Generated lepton asymmetry if one assumes a similar mass hierarchy for the right-handed neutrinos and the down-type quarks.*

scale $\Lambda_{\text{GUT}} \sim 10^{16}$ GeV, without any intermediate scale of symmetry breaking, which is natural in SO(10) unification. Alternatively, a Majorana mass scale of the order of 10^{12} to 10^{14} GeV can also be generated radiatively if SO(10) is broken into SU(5) at some high scale between 10^{16} GeV and the Planck-scale, and SU(5) is subsequently broken into the MSSM gauge group at the usual GUT scale $\sim 10^{16}$ GeV [21].

In eq. (49) we had assumed a mass hierarchy for the heavy Majorana neutrinos like for the up-type quarks. Alternatively, one can assume a weaker hierarchy, like for the down-type quarks by choosing

$$B = 10 \quad \text{and} \quad C = 3. \quad (65)$$

Keeping the other parameters in eq. (57) unchanged fixes the ν_e and ν_τ masses,

$$m_{\nu_e} \simeq 5 \cdot 10^{-6} \text{ eV}, \quad m_{\nu_\tau} \simeq 0.7 \text{ eV}, \quad (66)$$

and the mass parameter \widetilde{m}_1 ,

$$\widetilde{m}_1 \simeq 10^{-3} \text{ eV}. \quad (67)$$

Choosing the Dirac mass scale (60) we get a large Majorana mass scale

$$M_3 \simeq 4 \cdot 10^{13} \text{ GeV} \quad \Rightarrow \quad M_1 \simeq 4 \cdot 10^{10} \text{ GeV} \text{ and } M_2 \simeq 10^{12} \text{ GeV}. \quad (68)$$

From eq. (55) one obtains the CP asymmetry $\varepsilon_1 \simeq -6 \cdot 10^{-5}$. The corresponding solutions of the Boltzmann equations are shown in fig. 15. The final $(B - L)$ asymmetry,

$$Y_{B-L} \simeq 2 \cdot 10^{-8}, \quad (69)$$

is much larger than requested, but this value can always be lowered by adjusting the unknown phases. Hence, the possibility to generate a lepton asymmetry does not depend on the special form of the mass hierarchy assumed for the right-handed neutrinos.

In the non-supersymmetric scenario one finds for the same parameter choice

$$Y_{B-L} \simeq 2 \cdot 10^{-8} . \quad (70)$$

Hence, when comparing the supersymmetric and the non-supersymmetric scenario, one sees that the larger CP asymmetry in the former and the additional contributions from the sneutrino decays are compensated by the wash-out processes which are stronger than in the latter.

5 Conclusions

We conclude that the cosmological baryon asymmetry can be generated in a supersymmetric extension of the Standard Model by the out-of-equilibrium decays of heavy right-handed Majorana neutrinos and their scalar partners. Solving the Boltzmann equations we have shown that, in order to be consistent, one has to pay attention to two phenomena which can hamper the generation of a lepton asymmetry.

First, one has to take into consideration lepton number violating scatterings. These processes, which are usually neglected, can wash out a large part of the asymmetry if the Yukawa couplings of the right-handed neutrinos become too large.

On the other hand the neutrinos have to be brought into thermal equilibrium at high temperatures. We could show that for this purpose it is not necessary to assume additional interactions of the right-handed neutrinos in our theory, since the Yukawa interactions can be sufficiently strong to produce a thermal population of heavy neutrinos at high temperatures, while still being weak enough to prevent the final asymmetry from being washed out.

The observed baryon asymmetry can be obtained without any fine tuning of parameters if one assumes a similar pattern of mixings and Dirac masses for the neutrinos and the up-type quarks. Then the generated asymmetry is related to the ν_μ mass and fixing this mass to the value preferred by the MSW-solution to the solar neutrino problem leads to a baryon asymmetry of the requested order, provided $(B - L)$ is broken at the unification scale, as suggested by supersymmetric SO(10) unification.

In supersymmetric theories there are further possible sources of a $(B - L)$ asymmetry, e.g. it may be possible to combine inflation with leptogenesis (cf. refs. [22]). In this connection, possible constraints on the neutrino masses and on the reheating temperature from lepton number violating processes at low temperatures require further studies.

Acknowledgments

I would like to thank W. Buchmüller for many fruitful discussions and continuous support. It is also a pleasure to thank J. R. Espinosa for useful discussions. Finally, I would like to thank L. Covi, E. Roulet and F. Vissani for a helpful comment.

Appendix

A The Superfields

In addition to the usual MSSM particles the supersymmetric SO(10) contains right-handed neutrinos and their scalar partners. With $y = x - i\theta\sigma\bar{\theta}$ we have the following chiral superfields²

$$H_i = H_i(y) + \sqrt{2}\theta\widetilde{H}_i(y) + \theta\theta F_{H_i}(y), \quad (\text{A.1})$$

$$Q = \tilde{q}(y) + \sqrt{2}\theta q_L(y) + \theta\theta F_Q(y), \quad (\text{A.2})$$

$$L = \tilde{l}(y) + \sqrt{2}\theta l_L(y) + \theta\theta F_L(y), \quad (\text{A.3})$$

$$U^c = \widetilde{U}^c(y) + \sqrt{2}\theta u_R^c(y) + \theta\theta F_{U^c}(y), \quad (\text{A.4})$$

$$D^c = \widetilde{D}^c(y) + \sqrt{2}\theta d_R^c(y) + \theta\theta F_{D^c}(y), \quad (\text{A.5})$$

$$E^c = \widetilde{E}^c(y) + \sqrt{2}\theta e_R^c(y) + \theta\theta F_{E^c}(y), \quad (\text{A.6})$$

$$N^c = \widetilde{N}^c(y) + \sqrt{2}\theta\nu_R^c(y) + \theta\theta F_{N^c}(y). \quad (\text{A.7})$$

H_i denotes the two Higgs-doublets,

$$H_1 = \begin{pmatrix} H_1^0 \\ -H_1^- \end{pmatrix} \quad \text{and} \quad H_2 = \begin{pmatrix} H_2^+ \\ H_2^0 \end{pmatrix}, \quad (\text{A.8})$$

Q and L stand for the left-handed quark and lepton doublets and U^c , D^c , E^c and N^c are the right-handed singlet fields.

Besides the usual bispinors for the quarks and the charged leptons we can introduce Majorana-spinors for the right- and left-handed neutrinos

$$N = \begin{pmatrix} \nu_R^c{}_\alpha \\ \overline{\nu_R^c}{}^{\dot{\alpha}} \end{pmatrix} \quad \text{and} \quad \nu = \begin{pmatrix} \nu_{L\alpha} \\ \overline{\nu_L}{}^{\dot{\alpha}} \end{pmatrix}. \quad (\text{A.9})$$

In the symmetric phase of the MSSM no mixing occurs between the fermionic partners of gauge and Higgs bosons. Therefore, we have two Dirac higgsinos

$$\widetilde{h}^0 = \begin{pmatrix} \widetilde{H}_1^0{}_\alpha \\ \overline{\widetilde{H}_2^0}{}^{\dot{\alpha}} \end{pmatrix} \quad \text{and} \quad \widetilde{h}^- = \begin{pmatrix} \widetilde{H}_1^-{}_\alpha \\ \overline{\widetilde{H}_2^+}{}^{\dot{\alpha}} \end{pmatrix}, \quad (\text{A.10})$$

²We are using the conventions of ref. [23] with metric $\eta_{\mu\nu} = \text{diag}(1, -1, -1, -1)$.

which again form an isospin doublet,

$$\tilde{h} = \begin{pmatrix} \tilde{h}^0 \\ -\tilde{h}^- \end{pmatrix}. \quad (\text{A.11})$$

B Boltzmann equations

The microscopic evolution of particle densities and asymmetries is governed by a network of Boltzmann equations. In the following we will compile some basic formulae to introduce our notation³.

It is usually a good approximation to assume Maxwell-Boltzmann statistics, so that the equilibrium number density of a particle i is given by

$$n_i^{\text{eq}}(T) = \frac{g_i}{(2\pi)^3} \int d^3 p_i f_i^{\text{eq}} \quad \text{with} \quad f_i^{\text{eq}}(E_i, T) = e^{-E_i/T}, \quad (\text{B.1})$$

where g_i is the number of internal degrees of freedom. This particle density can be changed by interactions and by the expansion of the universe. Since we are only interested in the effect of the interactions it is useful to scale out the expansion. This is done by using the number of particles per comoving volume element,

$$Y_i = \frac{n_i}{s}, \quad (\text{B.2})$$

where s is the entropy density, as independent variable instead of the number density.

In our case elastic scatterings, which can only change the phase space distributions but not the particle densities, occur at a much higher rate than inelastic processes. Therefore, we can assume kinetic equilibrium, so that the phase space densities are given by

$$f_i(E_i, T) = \frac{n_i}{n_i^{\text{eq}}} e^{-E_i/T}. \quad (\text{B.3})$$

In this framework the Boltzmann equation describing the evolution of a particle number Y_ψ in an isentropically expanding universe reads [14,9]

$$\begin{aligned} \frac{dY_\psi}{dz} = & -\frac{z}{sH(m_\psi)} \sum_{a,i,j,\dots} \left[\frac{Y_\psi Y_a \dots}{Y_\psi^{\text{eq}} Y_a^{\text{eq}} \dots} \gamma^{\text{eq}}(\psi + a + \dots \rightarrow i + j + \dots) \right. \\ & \left. - \frac{Y_i Y_j \dots}{Y_i^{\text{eq}} Y_j^{\text{eq}} \dots} \gamma^{\text{eq}}(i + j + \dots \rightarrow \psi + a + \dots) \right], \quad (\text{B.4}) \end{aligned}$$

where $z = m_\psi/T$ and $H(m_\psi)$ is the Hubble parameter at $T = m_\psi$. The γ^{eq} are space time densities of scatterings for the different processes. For a decay one finds [9]

$$\gamma_D := \gamma^{\text{eq}}(\psi \rightarrow i + j + \dots) = n_\psi^{\text{eq}} \frac{K_1(z)}{K_2(z)} \Gamma, \quad (\text{B.5})$$

³For a review and references, see [14].

where K_1 and K_2 are modified Bessel functions and Γ is the usual decay width in the rest system of the decaying particle. Neglecting a possible CP violation, one finds the same reaction density for the inverse decay.

The reaction density for a two body scattering reads

$$\gamma^{\text{eq}}(\psi + a \leftrightarrow i + j + \dots) = \frac{T}{64\pi^4} \int_{(m_\psi+m_a)^2}^{\infty} ds \hat{\sigma}(s) \sqrt{s} K_1\left(\frac{\sqrt{s}}{T}\right), \quad (\text{B.6})$$

where s is the squared centre of mass energy and the reduced cross section $\hat{\sigma}(s)$ for the process $\psi + a \rightarrow i + j + \dots$ is related to the usual total cross section $\sigma(s)$ by

$$\hat{\sigma}(s) = \frac{8}{s} \left[(p_\psi \cdot p_a)^2 - m_\psi^2 m_a^2 \right] \sigma(s). \quad (\text{B.7})$$

C Reduced cross sections

In this section we will collect the reduced cross sections for all the $2 \leftrightarrow 2$ and $2 \leftrightarrow 3$ processes that we had discussed in section 2. The corresponding reaction densities, which can be calculated analytically in some interesting limiting cases, will be discussed in the next section.

C.1 Lepton number violating processes mediated by a right-handed neutrino

We have mentioned in the main text that we have to subtract the contributions coming from on-shell (s)neutrinos, i.e. we have to replace the usual propagators by off-shell propagators

$$\frac{1}{D_j(x)} := \frac{x - a_j}{(x - a_j)^2 + a_j c_j} \quad \text{and} \quad \frac{1}{\widetilde{D}_j(x)} := \frac{x - a_j}{(x - a_j)^2 + a_j \tilde{c}_j}. \quad (\text{C.1})$$

To begin with, let us specify the reduced cross sections for the reactions depicted in fig. 3. For the processes $\tilde{l} + \tilde{h} \leftrightarrow \tilde{l}^\dagger + \tilde{h}$ and $l + H_2 \leftrightarrow \bar{l} + H_2^\dagger$ one has

$$\begin{aligned} \hat{\sigma}_N^{(1)}(x) = \hat{\sigma}_N^{(2)}(x) = & \frac{1}{2\pi} \left\{ \sum_j (\lambda_\nu^\dagger \lambda_\nu)_{jj}^2 \frac{a_j}{x} \left[\frac{x}{a_j} + \frac{x}{D_j(x)} + \frac{x^2}{2D_j^2(x)} - \left(1 + \frac{x + a_j}{D_j(x)} \right) \ln \left(\frac{x + a_j}{a_j} \right) \right] \right. \\ & + \sum_{\substack{n,j \\ j < n}} \text{Re} \left[(\lambda_\nu^\dagger \lambda_\nu)_{nj}^2 \frac{\sqrt{a_n a_j}}{x} \left[\frac{x}{D_j(x)} + \frac{x}{D_n(x)} + \frac{x^2}{D_j(x) D_n(x)} \right. \right. \\ & \left. \left. + (x + a_j) \left(\frac{2}{a_n - a_j} - \frac{1}{D_n(x)} \right) \ln \left(\frac{x + a_j}{a_j} \right) + (x + a_n) \left(\frac{2}{a_j - a_n} - \frac{1}{D_j(x)} \right) \ln \left(\frac{x + a_n}{a_n} \right) \right] \right\}, \end{aligned} \quad (\text{C.2})$$

where n and j are the flavour indices of the neutrinos in the intermediate state. The interference terms with $n \neq j$ are always very small and can safely be neglected.

The reduced cross section for the process $\tilde{l} + \tilde{h} \leftrightarrow \bar{l} + H_2^\dagger$ reads

$$\begin{aligned} \hat{\sigma}_N^{(3)}(x) = & \frac{1}{2\pi} \left\{ \sum_j (\lambda_\nu^\dagger \lambda_\nu)_{jj}^2 \frac{a_j}{x} \left[\frac{-x}{x+a_j} + \frac{x}{D_j(x)} + \frac{x^2}{2D_j^2(x)} + \left(1 - \frac{a_j}{D_j(x)}\right) \ln \left(\frac{x+a_j}{a_j} \right) \right] \right. \\ & + \sum_{\substack{n,j \\ j < n}} \text{Re} \left[(\lambda_\nu^\dagger \lambda_\nu)_{nj}^2 \right] \frac{\sqrt{a_n a_j}}{x} \left[\frac{x}{D_j(x)} + \frac{x}{D_n(x)} + \frac{x^2}{D_j(x)D_n(x)} \right. \\ & \left. \left. - a_j \left(\frac{2}{a_n - a_j} + \frac{1}{D_n(x)} \right) \ln \left(\frac{x+a_j}{a_j} \right) - a_n \left(\frac{2}{a_j - a_n} + \frac{1}{D_j(x)} \right) \ln \left(\frac{x+a_n}{a_n} \right) \right] \right\}. \end{aligned} \quad (\text{C.3})$$

The same result is valid for the CP conjugated process.

For the process $l + \tilde{h} \leftrightarrow \tilde{l}^\dagger + H_2^\dagger$ one finds

$$\begin{aligned} \hat{\sigma}_N^{(4)}(x) = & \frac{1}{2\pi} \left\{ \sum_j (\lambda_\nu^\dagger \lambda_\nu)_{jj}^2 \frac{a_j}{x} \left[\frac{x^2}{a_j(x+a_j)} + \frac{x^2}{\widetilde{D}_j^2(x)} + \frac{x}{\widetilde{D}_j(x)} \ln \left(\frac{x+a_j}{a_j} \right) \right] \right. \\ & + \sum_{\substack{n,j \\ j < n}} \text{Re} \left[(\lambda_\nu^\dagger \lambda_\nu)_{nj}^2 \right] \frac{\sqrt{a_n a_j}}{x} \left[\frac{2x^2}{\widetilde{D}_j(x)\widetilde{D}_n(x)} + x \left(\frac{2}{a_n - a_j} + \frac{1}{\widetilde{D}_n(x)} \right) \ln \left(\frac{x+a_j}{a_j} \right) \right. \\ & \left. \left. + x \left(\frac{2}{a_j - a_n} + \frac{1}{\widetilde{D}_j(x)} \right) \ln \left(\frac{x+a_n}{a_n} \right) \right] \right\}. \end{aligned} \quad (\text{C.4})$$

For the scattering $\tilde{l} + H_2 \rightarrow \tilde{l}^\dagger + \widetilde{U}^c + \tilde{q}$ and the corresponding CP transformed process we have

$$\begin{aligned} \hat{\sigma}_N^{(5)}(x) = & \frac{3\alpha_u}{8\pi^2} \left\{ \sum_j (\lambda_\nu^\dagger \lambda_\nu)_{jj}^2 \frac{a_j}{x} \left[\frac{x}{a_j} + \frac{x}{\widetilde{D}_j(x)} + \frac{x^2}{\widetilde{D}_j^2(x)} - \left(1 + \frac{x+a_j}{\widetilde{D}_j(x)}\right) \ln \left(\frac{x+a_j}{a_j} \right) \right] \right. \\ & + \sum_{\substack{n,j \\ j < n}} \text{Re} \left[(\lambda_\nu^\dagger \lambda_\nu)_{nj}^2 \right] \frac{\sqrt{a_n a_j}}{x} \left[\frac{x}{\widetilde{D}_j(x)} + \frac{x}{\widetilde{D}_n(x)} + \frac{x^2}{\widetilde{D}_j(x)\widetilde{D}_n(x)} \right. \\ & \left. \left. + (x+a_j) \left(\frac{2}{a_n - a_j} - \frac{1}{\widetilde{D}_n(x)} \right) \ln \left(\frac{x+a_j}{a_j} \right) + (x+a_n) \left(\frac{2}{a_j - a_n} - \frac{1}{\widetilde{D}_j(x)} \right) \ln \left(\frac{x+a_n}{a_n} \right) \right] \right\}. \end{aligned} \quad (\text{C.5})$$

Finally, we have two processes which do not violate lepton number but merely transform leptons into scalar leptons and vice versa. We have the $2 \rightarrow 2$ scattering $l + H_2 \leftrightarrow \tilde{l} + \tilde{h}$,

$$\hat{\sigma}_N^{(6)}(x) = \frac{1}{4\pi} \sum_{j,n} \left| (\lambda_\nu^\dagger \lambda_\nu)_{nj} \right|^2 \frac{x^2}{D_j(x)D_n(x)}, \quad (\text{C.6})$$

and the $2 \rightarrow 3$ process $l + \tilde{h} \leftrightarrow \tilde{l} + \tilde{q}^\dagger + \widetilde{U}^{c\dagger}$,

$$\hat{\sigma}_N^{(7)}(x) = \frac{3\alpha_u}{16\pi^2} \sum_{j,n} \left| (\lambda_\nu^\dagger \lambda_\nu)_{nj} \right|^2 \frac{x^2}{\widetilde{D}_j(x)\widetilde{D}_n(x)}. \quad (\text{C.7})$$

Let us now come to the $2 \rightarrow 3$ processes shown in fig. 4.

For the transition $\tilde{q} + \widetilde{U}^c \rightarrow \tilde{l} + \tilde{l} + H_2$ the reduced cross section reads

$$\begin{aligned}
\hat{\sigma}_N^{(8)}(x) = & \frac{3\alpha_u}{16\pi^2} \left\{ \sum_j (\lambda_\nu^\dagger \lambda_\nu)_{jj}^2 \frac{a_j}{x} \left[-\frac{x}{a_j + \tilde{c}_j} + \frac{x - a_j}{\sqrt{a_j \tilde{c}_j}} \left[\arctan \left(\frac{x - a_j}{\sqrt{a_j \tilde{c}_j}} \right) + \arctan \left(\sqrt{\frac{a_j}{\tilde{c}_j}} \right) \right] \right. \right. \\
& \left. \left. - \ln \left(\frac{(x - a_j)^2 + a_j \tilde{c}_j}{a_j^2 + a_j \tilde{c}_j} \right) + \frac{1}{2} \int_0^x dx_1 \frac{1}{\tilde{D}_j(x_1)} \ln \left(\frac{(x - x_1 - a_j)^2 + a_j \tilde{c}_j}{a_j^2 + a_j \tilde{c}_j} \right) \right] \right. \\
& + 2 \sum_{\substack{n,j \\ j < n}} \text{Re} \left[(\lambda_\nu^\dagger \lambda_\nu)_{nj}^2 \frac{\sqrt{a_n a_j}}{x} \left[\frac{1}{2} \int_0^x dx_1 \frac{1}{\tilde{D}_n(x_1)} \ln \left(\frac{(x - x_1 - a_j)^2 + a_j \tilde{c}_j}{a_j^2 + a_j \tilde{c}_j} \right) \right. \right. \\
& + 2\sqrt{a_j \tilde{c}_j} \frac{x - a_n}{(a_j - a_n)^2} \left[\arctan \left(\frac{x - a_j}{\sqrt{a_j \tilde{c}_j}} \right) + \arctan \left(\sqrt{\frac{a_j}{\tilde{c}_j}} \right) \right] + \frac{x - a_j}{a_j - a_n} \ln \left(\frac{(x - a_j)^2 + a_j \tilde{c}_j}{a_j^2 + a_j \tilde{c}_j} \right) \\
& \left. \left. + 2\sqrt{a_n \tilde{c}_n} \frac{x - a_j}{(a_n - a_j)^2} \left[\arctan \left(\frac{x - a_n}{\sqrt{a_n \tilde{c}_n}} \right) + \arctan \left(\sqrt{\frac{a_n}{\tilde{c}_n}} \right) \right] + \frac{x - a_n}{a_n - a_j} \ln \left(\frac{(x - a_n)^2 + a_n \tilde{c}_n}{a_n^2 + a_n \tilde{c}_n} \right) \right] \right\}. \tag{C.8}
\end{aligned}$$

The remaining integral cannot be solved exactly. However, it can be neglected for $x > a_j, a_n$ and for $x < a_j, a_n$ it can be approximated by

$$\begin{aligned}
& \frac{1}{2} \int_0^x dx_1 \frac{1}{\tilde{D}_n(x_1)} \ln \left(\frac{(x - x_1 - a_j)^2 + a_j \tilde{c}_j}{a_j^2 + a_j \tilde{c}_j} \right) \\
& \approx \ln \left(\frac{a_j + a_n - x}{a_j} \right) \ln \left(\frac{a_n - x}{a_n} \right) + \text{Sp} \left(\frac{a_n}{a_n + a_j - x} \right) - \text{Sp} \left(\frac{a_n - x}{a_n + a_j - x} \right), \tag{C.9}
\end{aligned}$$

where $\text{Sp}(x)$ is the Spence function.

For the scatterings $\tilde{q} + \tilde{U}^c \rightarrow \tilde{l} + \tilde{l} + \tilde{h}$, $\tilde{l}^\dagger + \tilde{q} \rightarrow \tilde{l} + \tilde{U}^{c\dagger} + \tilde{h}$ and $\tilde{l}^\dagger + \tilde{U}^c \rightarrow \tilde{l} + \tilde{q}^\dagger + \tilde{h}$ the reduced cross sections are equal,

$$\begin{aligned}
\hat{\sigma}_N^{(9)}(x) = \hat{\sigma}_N^{(11)}(x) = & \frac{3\alpha_u}{8\pi^2 x} \left\{ \sum_j (\lambda_\nu^\dagger \lambda_\nu)_{jj}^2 \left[-\frac{3}{2}x + \frac{1}{2}(x - 2a_j) \ln \left(\frac{(x - a_j)^2 + a_j \tilde{c}_j}{a_j^2 + a_j \tilde{c}_j} \right) \right. \right. \\
& \left. \left. + \frac{1}{2} \sqrt{\frac{a_j}{\tilde{c}_j}} (x - a_j + 3\tilde{c}_j) \left[\arctan \left(\frac{x - a_j}{\sqrt{a_j \tilde{c}_j}} \right) + \arctan \left(\sqrt{\frac{a_j}{\tilde{c}_j}} \right) \right] \right] \right\} \\
& + 2 \sum_{\substack{n,j \\ j < n}} \left| (\lambda_\nu^\dagger \lambda_\nu)_{nj} \right|^2 \left[-2x + a_j \frac{x - a_j}{a_j - a_n} \ln \left(\frac{(x - a_j)^2 + a_j \tilde{c}_j}{a_j^2 + a_j \tilde{c}_j} \right) + a_n \frac{x - a_n}{a_n - a_j} \ln \left(\frac{(x - a_n)^2 + a_n \tilde{c}_n}{a_n^2 + a_n \tilde{c}_n} \right) \right. \\
& + 2\sqrt{a_j \tilde{c}_j} \frac{x a_n - 2a_n a_j + a_j^2}{(a_j - a_n)^2} \left[\arctan \left(\frac{x - a_j}{\sqrt{a_j \tilde{c}_j}} \right) + \arctan \left(\sqrt{\frac{a_j}{\tilde{c}_j}} \right) \right] \\
& \left. \left. + 2\sqrt{a_n \tilde{c}_n} \frac{x a_j - 2a_n a_j + a_n^2}{(a_n - a_j)^2} \left[\arctan \left(\frac{x - a_n}{\sqrt{a_n \tilde{c}_n}} \right) + \arctan \left(\sqrt{\frac{a_n}{\tilde{c}_n}} \right) \right] \right] \right\}. \tag{C.10}
\end{aligned}$$

For the process $\tilde{l}^\dagger + \tilde{q} \rightarrow \tilde{l} + \tilde{U}^{c\dagger} + H_2$ and similar reactions one gets

$$\begin{aligned}
\hat{\sigma}_N^{(10)}(x) &= \frac{3\alpha_u}{16\pi^2} \left\{ \sum_j (\lambda_\nu^\dagger \lambda_\nu)_{jj}^2 \frac{a_j}{x} \left[\frac{x}{a_j} - 2 \ln \left(\frac{x+a_j}{a_j} \right) - \ln \left(\frac{(x-a_j)^2 + a_j \tilde{c}_j}{a_j^2 + a_j \tilde{c}_j} \right) \right] \right. \\
&\quad + \frac{x-a_j}{\sqrt{a_j \tilde{c}_j}} \left[\arctan \left(\frac{x-a_j}{\sqrt{a_j \tilde{c}_j}} \right) + \arctan \left(\sqrt{\frac{a_j}{\tilde{c}_j}} \right) \right] + 2 \int_0^x dx_1 \frac{1}{\tilde{D}_j(x_1)} \left[\text{Sp} \left(-\frac{x}{a_j} \right) - \text{Sp} \left(-\frac{x_1}{a_j} \right) \right] \Bigg\} \\
&\quad + 2 \sum_{\substack{n,j \\ j < n}} \text{Re} \left[(\lambda_\nu^\dagger \lambda_\nu)_{nj}^2 \frac{\sqrt{a_n a_j}}{x} \left[2 \frac{x+a_j}{a_n - a_j} \ln \left(\frac{x+a_j}{a_j} \right) + 2 \frac{x+a_n}{a_j - a_n} \ln \left(\frac{x+a_n}{a_n} \right) \right] \right. \\
&\quad + \frac{x-a_j}{a_j - a_n} \ln \left(\frac{(x-a_j)^2 + a_j \tilde{c}_j}{a_j^2 + a_j \tilde{c}_j} \right) + 2 \sqrt{a_j \tilde{c}_j} \frac{x-a_n}{(a_j - a_n)^2} \left[\arctan \left(\frac{x-a_j}{\sqrt{a_j \tilde{c}_j}} \right) + \arctan \left(\sqrt{\frac{a_j}{\tilde{c}_j}} \right) \right] \\
&\quad + \frac{x-a_n}{a_n - a_j} \ln \left(\frac{(x-a_n)^2 + a_n \tilde{c}_n}{a_n^2 + a_n \tilde{c}_n} \right) + 2 \sqrt{a_n \tilde{c}_n} \frac{x-a_j}{(a_n - a_j)^2} \left[\arctan \left(\frac{x-a_n}{\sqrt{a_n \tilde{c}_n}} \right) + \arctan \left(\sqrt{\frac{a_n}{\tilde{c}_n}} \right) \right] \\
&\quad \left. + \int_0^x dx_1 \left[\frac{1}{\tilde{D}_j(x_1)} \left(\text{Sp} \left(-\frac{x}{a_n} \right) - \text{Sp} \left(-\frac{x_1}{a_n} \right) \right) + \frac{1}{\tilde{D}_n(x_1)} \left(\text{Sp} \left(-\frac{x}{a_j} \right) - \text{Sp} \left(-\frac{x_1}{a_j} \right) \right) \right] \right\}. \tag{C.11}
\end{aligned}$$

The remaining integral can again not be solved exactly. However it can be approximated by

$$\begin{aligned}
&\int_0^x dx_1 \frac{1}{\tilde{D}_j(x_1)} \left[\text{Sp} \left(-\frac{x}{a_n} \right) - \text{Sp} \left(-\frac{x_1}{a_n} \right) \right] \\
&\approx \frac{x}{a_n} - \frac{\sqrt{a_j \tilde{c}_j}}{a_n} \left[\arctan \left(\frac{x-a_j}{\sqrt{a_j \tilde{c}_j}} \right) + \arctan \left(\sqrt{\frac{a_j}{\tilde{c}_j}} \right) \right] - \frac{x-a_j}{2a_n} \ln \left(\frac{(x-a_j)^2 + a_j \tilde{c}_j}{a_j^2 + a_j \tilde{c}_j} \right)
\end{aligned} \tag{C.12}$$

for $x < a_n$ and for $x > a_n$ it can be neglected.

Finally, we have to compute the t - and u -channel processes from fig. 5 which give comparatively simple contributions.

For the processes $\tilde{l} + \tilde{l} \leftrightarrow \tilde{h} + \tilde{h}$ and $l + l \leftrightarrow H_2^\dagger + H_2^\dagger$ we get

$$\begin{aligned}
\hat{\sigma}_N^{(12)}(x) &= \hat{\sigma}_N^{(13)}(x) = \frac{1}{2\pi} \left\{ \sum_j (\lambda_\nu^\dagger \lambda_\nu)_{jj}^2 \left[\frac{x}{x+a_j} + \frac{a_j}{x+2a_j} \ln \left(\frac{x+a_j}{a_j} \right) \right] \right. \\
&\quad + \sum_{\substack{n,j \\ j < n}} \text{Re} \left[(\lambda_\nu^\dagger \lambda_\nu)_{nj}^2 \sqrt{a_n a_j} \left[\left(\frac{1}{x+a_n+a_j} + \frac{2}{a_n-a_j} \right) \ln \left(\frac{x+a_j}{a_j} \right) \right. \right. \\
&\quad \left. \left. + \left(\frac{1}{x+a_n+a_j} + \frac{2}{a_j-a_n} \right) \ln \left(\frac{x+a_n}{a_n} \right) \right] \right\}. \tag{C.13}
\end{aligned}$$

At this order of perturbation theory the same result is valid for the CP transformed processes.

For the scattering $\tilde{l} + l \leftrightarrow \tilde{h} + H_2^\dagger$ one has

$$\begin{aligned} \hat{\sigma}_N^{(14)}(x) &= \frac{1}{2\pi} \left\{ \sum_j (\lambda_\nu^\dagger \lambda_\nu)_{jj}^2 \left[\frac{x}{x+a_j} - \frac{a_j}{x+2a_j} \ln \left(\frac{x+a_j}{a_j} \right) \right] \right. \\ &\quad + 2 \sum_{\substack{n,j \\ j < n}} \text{Re} \left[(\lambda_\nu^\dagger \lambda_\nu)_{nj}^2 \right] \sqrt{a_n a_j} \left[\left(\frac{1}{x+a_n+a_j} + \frac{1}{a_n-a_j} \right) \ln \left(\frac{x+a_j}{a_j} \right) \right. \\ &\quad \left. \left. + \left(\frac{1}{x+a_n+a_j} + \frac{1}{a_j-a_n} \right) \ln \left(\frac{x+a_n}{a_n} \right) \right] \right\}. \end{aligned} \quad (\text{C.14})$$

The $2 \rightarrow 3$ process $H_2 + \tilde{q}^\dagger \leftrightarrow \tilde{l}^\dagger + \tilde{l}^\dagger + \tilde{U}^c$ gives

$$\begin{aligned} \hat{\sigma}_N^{(15)}(x) &= \frac{3\alpha_u}{8\pi^2} \left\{ \sum_j (\lambda_\nu^\dagger \lambda_\nu)_{jj}^2 \frac{a_j}{x} \left[\frac{x}{a_j} - \left(1 - \frac{1}{2} \ln \left(\frac{x+2a_j}{a_j} \right) \right) \ln \left(\frac{x+a_j}{a_j} \right) \right. \right. \\ &\quad \left. \left. + \frac{1}{2} \text{Sp} \left(\frac{a_j}{x+2a_j} \right) - \frac{1}{2} \text{Sp} \left(\frac{x+a_j}{x+2a_j} \right) \right] \right. \\ &\quad + \sum_{\substack{n,j \\ j < n}} \text{Re} \left[(\lambda_\nu^\dagger \lambda_\nu)_{nj}^2 \right] \frac{\sqrt{a_n a_j}}{x} \left[\left(2 \frac{x+a_j}{a_n-a_j} + \ln \left(\frac{x+a_n+a_j}{a_n} \right) \right) \ln \left(\frac{x+a_j}{a_j} \right) \right. \\ &\quad \left. \left. + \left(2 \frac{x+a_n}{a_j-a_n} + \ln \left(\frac{x+a_n+a_j}{a_j} \right) \right) \ln \left(\frac{x+a_n}{a_n} \right) \right] \right. \\ &\quad \left. + \text{Sp} \left(\frac{a_j}{x+a_n+a_j} \right) - \text{Sp} \left(\frac{x+a_j}{x+a_n+a_j} \right) + \text{Sp} \left(\frac{an}{x+a_n+a_j} \right) - \text{Sp} \left(\frac{x+an}{x+a_n+a_j} \right) \right] \right\}. \end{aligned} \quad (\text{C.15})$$

For the related transition $\tilde{l} + \tilde{l} \leftrightarrow \tilde{U}^c + \tilde{q} + H_2^\dagger$ we have

$$\begin{aligned} \hat{\sigma}_N^{(16)}(x) &= \frac{3\alpha_u}{16\pi^2} \left\{ \sum_j (\lambda_\nu^\dagger \lambda_\nu)_{jj}^2 \frac{a_j}{x} \left[\frac{x}{a_j} + 2 \text{Sp} \left(-\frac{x+a_j}{a_j} \right) + \frac{\pi^2}{6} \right. \right. \\ &\quad \left. \left. - \left(1 - 2 \ln \left(\frac{x+2a_j}{a_j} \right) \right) \ln \left(\frac{x+a_j}{a_j} \right) \right] \right. \\ &\quad + 2 \sum_{\substack{n,j \\ j < n}} \text{Re} \left[(\lambda_\nu^\dagger \lambda_\nu)_{nj}^2 \right] \frac{\sqrt{a_n a_j}}{x} \left[\left(\frac{x+a_j}{a_n-a_j} + \ln \left(\frac{x+a_n+a_j}{a_n} \right) \right) \ln \left(\frac{x+a_j}{a_j} \right) + \text{Sp} \left(-\frac{x+a_j}{a_n} \right) \right. \\ &\quad \left. \left. + \left(\frac{x+a_n}{a_j-a_n} + \ln \left(\frac{x+a_n+a_j}{a_j} \right) \right) \ln \left(\frac{x+a_n}{a_n} \right) + \text{Sp} \left(-\frac{x+a_n}{a_j} \right) + \frac{\pi^2}{6} + \frac{1}{2} \ln^2 \left(\frac{a_n}{a_j} \right) \right] \right\}. \end{aligned} \quad (\text{C.16})$$

There are some $2 \rightarrow 2$ processes left which do not violate lepton number but simply transform leptons into scalar leptons, like in the process $\tilde{l} + \tilde{l} \leftrightarrow \tilde{h} + H_2$

$$\begin{aligned} \hat{\sigma}_N^{(17)}(x) &= \frac{1}{2\pi} \left\{ \sum_j (\lambda_\nu^\dagger \lambda_\nu)_{jj}^2 \left[\frac{-x}{x+a_j} + \ln \left(\frac{x+a_j}{a_j} \right) \right] \right. \\ &\quad \left. + 2 \sum_{\substack{n,j \\ j < n}} \left| (\lambda_\nu^\dagger \lambda_\nu)_{nj} \right|^2 \left[\frac{a_j}{a_j-a_n} \ln \left(\frac{x+a_j}{a_j} \right) + \frac{a_n}{a_n-a_j} \ln \left(\frac{x+a_n}{a_n} \right) \right] \right\}, \end{aligned} \quad (\text{C.17})$$

or in the similar process $\tilde{l} + H_2^\dagger \leftrightarrow \tilde{h} + l$

$$\begin{aligned} \hat{\sigma}_N^{(18)}(x) = & \frac{1}{2\pi} \left\{ \sum_j (\lambda_\nu^\dagger \lambda_\nu)_{jj}^2 \left[-2 + \frac{x+2a_j}{x} \ln \left(\frac{x+a_j}{a_j} \right) \right] \right. \\ & \left. + 2 \sum_{\substack{n,j \\ j < n}} \left| (\lambda_\nu^\dagger \lambda_\nu)_{nj} \right|^2 \left[-1 + \frac{a_j}{x} \frac{x+a_j}{a_j - a_n} \ln \left(\frac{x+a_j}{a_j} \right) + \frac{a_n}{x} \frac{x+a_n}{a_n - a_j} \ln \left(\frac{x+a_n}{a_n} \right) \right] \right\}. \end{aligned} \quad (\text{C.18})$$

Finally, the last process $l + \tilde{l}^\dagger \leftrightarrow \tilde{h} + \tilde{q}^\dagger + \tilde{U}^{c\dagger}$ gives

$$\begin{aligned} \hat{\sigma}_N^{(19)}(x) = & \frac{3\alpha_u}{8\pi^2} \left\{ \sum_j (\lambda_\nu^\dagger \lambda_\nu)_{jj}^2 \left[-2 + \frac{x+2a_j}{x} \ln \left(\frac{x+a_j}{a_j} \right) \right] \right. \\ & \left. + 2 \sum_{\substack{n,j \\ j < n}} \left| (\lambda_\nu^\dagger \lambda_\nu)_{nj} \right|^2 \left[-1 + \frac{a_j}{x} \frac{x+a_j}{a_j - a_n} \ln \left(\frac{x+a_j}{a_j} \right) + \frac{a_n}{x} \frac{x+a_n}{a_n - a_j} \ln \left(\frac{x+a_n}{a_n} \right) \right] \right\}. \end{aligned} \quad (\text{C.19})$$

C.2 Scattering off a top or a stop

For the processes specified in fig. 6 the reduced cross sections read

$$\hat{\sigma}_{t_j}^{(0)} = \frac{3\alpha_u}{2} (\lambda_\nu^\dagger \lambda_\nu)_{jj} \frac{x^2 - a_j^2}{x^2}, \quad (\text{C.20})$$

$$\hat{\sigma}_{t_j}^{(1)} = 3\alpha_u (\lambda_\nu^\dagger \lambda_\nu)_{jj} \frac{x - a_j}{x} \left[-\frac{2x - a_j + 2a_h}{x - a_j + a_h} + \frac{x + 2a_h}{x - a_j} \ln \left(\frac{x - a_j + a_h}{a_h} \right) \right], \quad (\text{C.21})$$

$$\hat{\sigma}_{t_j}^{(2)} = 3\alpha_u (\lambda_\nu^\dagger \lambda_\nu)_{jj} \frac{x - a_j}{x} \left[-\frac{x - a_j}{x - a_j + 2a_h} + \ln \left(\frac{x - a_j + a_h}{a_h} \right) \right], \quad (\text{C.22})$$

$$\hat{\sigma}_{t_j}^{(3)} = 3\alpha_u (\lambda_\nu^\dagger \lambda_\nu)_{jj} \left(\frac{x - a_j}{x} \right)^2, \quad (\text{C.23})$$

$$\hat{\sigma}_{t_j}^{(4)} = 3\alpha_u (\lambda_\nu^\dagger \lambda_\nu)_{jj} \frac{x - a_j}{x} \left[\frac{x - 2a_j + 2a_h}{x - a_j + a_h} + \frac{a_j - 2a_h}{x - a_j} \ln \left(\frac{x - a_j + a_h}{a_h} \right) \right]. \quad (\text{C.24})$$

To regularize an infrared divergence in the t -channel diagrams we had to introduce a Higgs-mass

$$a_h := \left(\frac{\mu}{M_1} \right)^2. \quad (\text{C.25})$$

In the calculations we have used the value $\mu = 800$ GeV.

The analogous processes involving a scalar neutrino (cf. fig. 7) give similar contributions

$$\hat{\sigma}_{t_j}^{(5)} = \frac{3\alpha_u}{2} (\lambda_\nu^\dagger \lambda_\nu)_{jj} \left(\frac{x - a_j}{x} \right)^2, \quad (\text{C.26})$$

$$\hat{\sigma}_{t_j}^{(6)} = 3\alpha_u (\lambda_\nu^\dagger \lambda_\nu)_{jj} \frac{x - a_j}{x} \left[-2 + \frac{x - a_j + 2a_h}{x - a_j} \ln \left(\frac{x - a_j + a_h}{a_h} \right) \right], \quad (\text{C.27})$$

$$\hat{\sigma}_{t_j}^{(7)} = 3\alpha_u (\lambda_\nu^\dagger \lambda_\nu)_{jj} \left[-\frac{x-a_j}{x-a_j+2a_h} + \ln\left(\frac{x-a_j+a_h}{a_h}\right) \right], \quad (\text{C.28})$$

$$\hat{\sigma}_{t_j}^{(8)} = 3\alpha_u (\lambda_\nu^\dagger \lambda_\nu)_{jj} \frac{x-a_j}{x} \frac{a_j}{x}, \quad (\text{C.29})$$

$$\hat{\sigma}_{t_j}^{(9)} = 3\alpha_u (\lambda_\nu^\dagger \lambda_\nu)_{jj} \frac{a_j}{x} \left[-\frac{x-a_j}{x-a_j+a_h} + \ln\left(\frac{x-a_j+a_h}{a_h}\right) \right]. \quad (\text{C.30})$$

C.3 Neutrino pair creation and annihilation

With the abbreviations

$$\lambda_{ij} = \lambda(x, a_i, a_j) = \left[x - (\sqrt{a_i} + \sqrt{a_j})^2 \right] \left[x - (\sqrt{a_i} - \sqrt{a_j})^2 \right] \quad (\text{C.31})$$

$$L_{ij} = \ln\left(\frac{x-a_i-a_j+\sqrt{\lambda_{ij}}}{x-a_i-a_j-\sqrt{\lambda_{ij}}}\right), \quad (\text{C.32})$$

the reduced cross sections for the right-handed neutrino pair creation read

$$\hat{\sigma}_{N_i N_j}^{(1)} = \frac{1}{4\pi} \left\{ (\lambda_\nu^\dagger \lambda_\nu)_{jj} (\lambda_\nu^\dagger \lambda_\nu)_{ii} \left[-\frac{2}{x} \sqrt{\lambda_{ij}} + L_{ij} \right] - 2 \operatorname{Re} \left[(\lambda_\nu^\dagger \lambda_\nu)_{ji}^2 \right] \frac{\sqrt{a_i a_j} (a_i + a_j)}{x(x-a_i-a_j)} L_{ij} \right\}, \quad (\text{C.33})$$

$$\hat{\sigma}_{N_i N_j}^{(2)} = \frac{1}{4\pi} \left\{ (\lambda_\nu^\dagger \lambda_\nu)_{jj} (\lambda_\nu^\dagger \lambda_\nu)_{ii} \left[\frac{2}{x} \sqrt{\lambda_{ij}} + \frac{a_i + a_j}{x} L_{ij} \right] - 2 \operatorname{Re} \left[(\lambda_\nu^\dagger \lambda_\nu)_{ji}^2 \right] \frac{\sqrt{a_i a_j}}{x-a_i-a_j} L_{ij} \right\} \quad (\text{C.34})$$

$$\hat{\sigma}_{N_i N_j}^{(3)} = \frac{1}{4\pi} \left\{ \left| (\lambda_\nu^\dagger \lambda_\nu)_{ji} \right|^2 \left[-\frac{2}{x} \sqrt{\lambda_{ij}} + L_{ij} \right] - 2 \operatorname{Re} \left[(\lambda_\nu^\dagger \lambda_\nu)_{ji}^2 \right] \frac{\sqrt{a_i a_j} (a_i + a_j)}{x(x-a_i-a_j)} L_{ij} \right\}, \quad (\text{C.35})$$

$$\hat{\sigma}_{N_i N_j}^{(4)} = \frac{1}{4\pi} \left\{ \left| (\lambda_\nu^\dagger \lambda_\nu)_{ji} \right|^2 \left[\frac{2}{x} \sqrt{\lambda_{ij}} + \frac{a_i + a_j}{x} L_{ij} \right] - 2 \operatorname{Re} \left[(\lambda_\nu^\dagger \lambda_\nu)_{ji}^2 \right] \frac{\sqrt{a_i a_j}}{x-a_i-a_j} L_{ij} \right\}. \quad (\text{C.36})$$

For the scalar neutrinos one has similarly

$$\hat{\sigma}_{\widetilde{N}_i^c \widetilde{N}_j^c}^{(1)} = \frac{1}{4\pi} (\lambda_\nu^\dagger \lambda_\nu)_{jj} (\lambda_\nu^\dagger \lambda_\nu)_{ii} \left[-\frac{2}{x} \sqrt{\lambda_{ij}} + \frac{x-a_i-a_j}{x} L_{ij} \right], \quad (\text{C.37})$$

$$\hat{\sigma}_{\widetilde{N}_i^c \widetilde{N}_j^c}^{(2)} = \frac{1}{4\pi} \left\{ (\lambda_\nu^\dagger \lambda_\nu)_{jj} (\lambda_\nu^\dagger \lambda_\nu)_{ii} \frac{2}{x} \sqrt{\lambda_{ij}} - 2 \operatorname{Re} \left[(\lambda_\nu^\dagger \lambda_\nu)_{ji}^2 \right] \frac{\sqrt{a_i a_j}}{x} L_{ij} \right\}, \quad (\text{C.38})$$

$$\hat{\sigma}_{\widetilde{N}_i^c \widetilde{N}_j^c}^{(3)} = \frac{1}{4\pi} \left| (\lambda_\nu^\dagger \lambda_\nu)_{ji} \right|^2 \left[-\frac{2}{x} \sqrt{\lambda_{ij}} + \frac{x-a_i-a_j}{x} L_{ij} \right], \quad (\text{C.39})$$

$$\hat{\sigma}_{\widetilde{N}_i^c \widetilde{N}_j^c}^{(4)} = \frac{1}{4\pi} \left\{ \left| (\lambda_\nu^\dagger \lambda_\nu)_{ji} \right|^2 \frac{2}{x} \sqrt{\lambda_{ij}} - 2 \operatorname{Re} \left[(\lambda_\nu^\dagger \lambda_\nu)_{ji}^2 \right] \frac{\sqrt{a_i a_j}}{x} L_{ij} \right\}. \quad (\text{C.40})$$

For the diagrams involving one neutrino and one sneutrino (cf. fig. 10) one finally has

$$\hat{\sigma}_{N_j \widetilde{N}_i^c}^{(1)} = \frac{1}{4\pi} \left\{ (\lambda_\nu^\dagger \lambda_\nu)_{jj} (\lambda_\nu^\dagger \lambda_\nu)_{ii} \frac{x+a_i-a_j}{x} L_{ij} - 2 \operatorname{Re} \left[(\lambda_\nu^\dagger \lambda_\nu)_{ji}^2 \right] \frac{\sqrt{a_i a_j}}{x} \frac{x+a_i-a_j}{x-a_i-a_j} L_{ij} \right\} \quad (\text{C.41})$$

$$\hat{\sigma}_{N_j \widetilde{N}_i^c}^{(2)} = \frac{1}{4\pi} \left\{ \left| (\lambda_\nu^\dagger \lambda_\nu)_{ji} \right|^2 \frac{x+a_i-a_j}{x} L_{ij} - 2 \operatorname{Re} \left[(\lambda_\nu^\dagger \lambda_\nu)_{ji}^2 \right] \frac{\sqrt{a_i a_j}}{x} \frac{x+a_i-a_j}{x-a_i-a_j} L_{ij} \right\}. \quad (\text{C.42})$$

D Reaction densities

In general the reaction densities corresponding to the reduced cross sections discussed in appendix C have to be calculated numerically. However, there exist some interesting limiting cases where one can calculate them analytically.

D.1 Lepton number violating scatterings

In the Boltzmann equations we do not need every reaction density $\gamma_N^{(i)}$, $i = 1, \dots, 19$ separately (cf. sect. 3.1). We only have to consider the combined reaction densities

$$\gamma_A^{\Delta L} = 2\gamma_N^{(1)} + \gamma_N^{(3)} + \gamma_N^{(4)} + \gamma_N^{(6)} + \gamma_N^{(7)} + 2\gamma_N^{(12)} + \gamma_N^{(14)}, \quad (\text{D.1})$$

$$\gamma_B^{\Delta L} = \gamma_N^{(3)} + \gamma_N^{(4)} - \gamma_N^{(6)} - \gamma_N^{(7)} + \gamma_N^{(14)}, \quad (\text{D.2})$$

$$\gamma_C^{\Delta L} = 3\gamma_N^{(9)} + \gamma_N^{(17)} + \gamma_N^{(18)} + 6\gamma_N^{(19)}, \quad (\text{D.3})$$

$$\gamma_D^{\Delta L} = 4\gamma_N^{(5)} + 2\gamma_N^{(8)} + 8\gamma_N^{(10)} + 3\gamma_N^{(9)} + 4\gamma_N^{(15)} + 2\gamma_N^{(16)} + \gamma_N^{(17)} + \gamma_N^{(18)} + 6\gamma_N^{(19)}. \quad (\text{D.4})$$

For low temperatures, i.e. $z \gg 1/\sqrt{a_j}$, the dominant contribution to the integrand of the reaction densities comes from small centre of mass energies, i.e. $x \ll a_j$. In this limit the reduced cross sections $\hat{\sigma}_N^{(i)}$ for the $L + \tilde{L}$ violating or conserving processes behave differently. For the $L + \tilde{L}$ violating scatterings ($i = 1, \dots, 5, 8, 10, 12, \dots, 16$) one finds

$$\hat{\sigma}_N^{(i)} \propto x \quad \text{for } x \ll a_j, \quad (\text{D.5})$$

while one has

$$\hat{\sigma}_N^{(i)} \propto x^2 \quad \text{for } x \ll a_j \quad (\text{D.6})$$

for the $L + \tilde{L}$ conserving processes ($i = 6, 7, 9, 11, 17, 18, 19$). Hence, the reaction densities can be calculated analytically in this limit and one finds

$$\gamma_A^{\Delta L} = \frac{M_1^4}{\pi^5} \frac{1}{z^6} \left\{ \sum_j (\lambda_\nu^\dagger \lambda_\nu)_{jj}^2 \frac{2}{a_j} + \sum_{\substack{n,j \\ j < n}} \text{Re} \left[(\lambda_\nu^\dagger \lambda_\nu)_{nj}^2 \right] \frac{19}{4\sqrt{a_n a_j}} \right\}, \quad (\text{D.7})$$

$$\gamma_B^{\Delta L} = \frac{M_1^4}{\pi^5} \frac{1}{z^6} \left\{ \sum_j (\lambda_\nu^\dagger \lambda_\nu)_{jj}^2 \frac{1}{2a_j} + \sum_{\substack{n,j \\ j < n}} \text{Re} \left[(\lambda_\nu^\dagger \lambda_\nu)_{nj}^2 \right] \frac{7}{4\sqrt{a_n a_j}} \right\}, \quad (\text{D.8})$$

$$\gamma_C^{\Delta L} = \frac{M_1^4}{\pi^5} \frac{1}{z^8} \left\{ \sum_j (\lambda_\nu^\dagger \lambda_\nu)_{jj}^2 \frac{1}{a_j^2} \left(4 + \frac{27\alpha_u}{4\pi} \right) + \sum_{\substack{n,j \\ j < n}} \left| (\lambda_\nu^\dagger \lambda_\nu)_{nj} \right|^2 \frac{1}{a_j a_n} \left(8 + \frac{18\alpha_u}{\pi} \right) \right\}, \quad (\text{D.9})$$

$$\gamma_D^{\Delta L} = \frac{M_1^4}{\pi^5} \frac{\alpha_u}{\pi} \frac{1}{z^6} \left\{ \sum_j (\lambda_\nu^\dagger \lambda_\nu)_{jj}^2 \frac{153}{32a_j} + \sum_{\substack{n,j \\ j < n}} \text{Re} \left[(\lambda_\nu^\dagger \lambda_\nu)_{nj}^2 \right] \frac{147}{16\sqrt{a_n a_j}} \right\}. \quad (\text{D.10})$$

For high temperatures, i.e. $z \ll 1/\sqrt{a_j}$, we can use the asymptotic expansions of the reduced cross sections to compute the reactions densities and we get

$$\begin{aligned} \gamma_A^{\Delta L} = & \frac{M_1^4}{64\pi^5} \frac{1}{z^4} \left\{ \left(13 + \frac{3\alpha_u}{4\pi}\right) \sum_j (\lambda_\nu^\dagger \lambda_\nu)_{jj}^2 + \sum_{\substack{n,j \\ j < n}} \text{Re} \left[(\lambda_\nu^\dagger \lambda_\nu)_{nj}^2 \right] \frac{24\sqrt{a_n a_j}}{a_n - a_j} \ln \left(\frac{a_n}{a_j} \right) \right. \\ & \left. + \left(2 + \frac{3\alpha_u}{2\pi}\right) \sum_{\substack{n,j \\ j < n}} \left| (\lambda_\nu^\dagger \lambda_\nu)_{nj} \right|^2 \right\}, \end{aligned} \quad (\text{D.11})$$

$$\begin{aligned} \gamma_B^{\Delta L} = & \frac{M_1^4}{64\pi^5} \frac{1}{z^4} \left\{ \left(3 - \frac{3\alpha_u}{4\pi}\right) \sum_j (\lambda_\nu^\dagger \lambda_\nu)_{jj}^2 + \sum_{\substack{n,j \\ j < n}} \text{Re} \left[(\lambda_\nu^\dagger \lambda_\nu)_{nj}^2 \right] \frac{8\sqrt{a_n a_j}}{a_n - a_j} \ln \left(\frac{a_n}{a_j} \right) \right. \\ & \left. - \left(2 + \frac{3\alpha_u}{2\pi}\right) \sum_{\substack{n,j \\ j < n}} \left| (\lambda_\nu^\dagger \lambda_\nu)_{nj} \right|^2 \right\}, \end{aligned} \quad (\text{D.12})$$

$$\begin{aligned} \gamma_C^{\Delta L} = & \frac{M_1^4}{32\pi^5} \frac{1}{z^4} \left\{ \sum_j (\lambda_\nu^\dagger \lambda_\nu)_{jj}^2 \left[-1 - \frac{45\alpha_u}{8\pi} + \frac{9\alpha_u}{8} \sqrt{\frac{a_j}{\tilde{c}_j}} + \left(4 + \frac{27\alpha_u}{2\pi}\right) \left(\ln \left(\frac{2}{z\sqrt{a_j}} \right) - \gamma_E \right) \right] \right. \\ & + \sum_{\substack{n,j \\ j < n}} \left| (\lambda_\nu^\dagger \lambda_\nu)_{nj} \right|^2 \left[2 + \frac{9\alpha_u}{(a_n - a_j)^2} \left(a_n \sqrt{a_j \tilde{c}_j} + a_j \sqrt{a_n \tilde{c}_n} \right) \right. \\ & \left. \left. + \left(8 + \frac{36\alpha_u}{\pi}\right) \left(\frac{a_n}{a_n - a_j} \ln \left(\frac{2}{\sqrt{a_n} z} \right) + \frac{a_j}{a_j - a_n} \ln \left(\frac{2}{\sqrt{a_j} z} \right) - \gamma_E \right) \right] \right\}, \end{aligned} \quad (\text{D.13})$$

$$\begin{aligned} \gamma_D^{\Delta L} = & \frac{M_1^4}{32\pi^5} \frac{1}{z^4} \left\{ \sum_j (\lambda_\nu^\dagger \lambda_\nu)_{jj}^2 \left[-1 + \frac{27\alpha_u}{8\pi} + \frac{39\alpha_u}{8} \sqrt{\frac{a_j}{\tilde{c}_j}} + \left(4 + \frac{27\alpha_u}{2\pi}\right) \left(\ln \left(\frac{2}{z\sqrt{a_j}} \right) - \gamma_E \right) \right] \right. \\ & + \sum_{\substack{n,j \\ j < n}} \left| (\lambda_\nu^\dagger \lambda_\nu)_{nj} \right|^2 \left[4 - 8\gamma_E + \frac{8}{a_n - a_j} \left(a_n \ln \left(\frac{2}{\sqrt{a_n} z} \right) - a_j \ln \left(\frac{2}{\sqrt{a_j} z} \right) \right) \right] \\ & \left. + \frac{3\alpha_u}{\pi} \sum_{\substack{n,j \\ j < n}} \text{Re} \left[(\lambda_\nu^\dagger \lambda_\nu)_{nj}^2 \right] \sqrt{a_n a_j} \left[\frac{7}{2} \frac{1}{a_n - a_j} \ln \left(\frac{a_n}{a_j} \right) + \frac{5\pi}{(a_n - a_j)^2} \left(\sqrt{a_j \tilde{c}_j} + \sqrt{a_n \tilde{c}_n} \right) \right] \right\}, \end{aligned} \quad (\text{D.14})$$

where $\gamma_E = 0.577216$ is Euler's constant. These reaction densities are therefore proportional to T^4 at high temperatures, as expected on purely dimensional grounds.

For intermediate temperatures $z \sim 1/\sqrt{a_j}$ the reaction densities have to be computed numerically. This becomes increasingly difficult in the narrow width limit, where $1/D_j(x)$ has two very sharp peaks. However, in the limit $c_j \rightarrow 0$ the two peaks in $1/D_j(x)$ cancel each other, since they have a different sign, while the peaks in $1/D_j^2(x)$ add up. Therefore, the terms proportional to $1/D_j(x)$ or $1/D_j(x)D_n(x)$ with $n \neq j$ can be neglected in the narrow width

limit, while $1/D_j^2(x)$ can be approximated by a δ -function

$$\frac{1}{D_j^2(x)} \approx \frac{\pi}{2\sqrt{a_j c_j}} \delta(x - a_j) . \quad (\text{D.15})$$

An analogous relation holds for $1/\widetilde{D}_j^2(x)$.

These relations allow to calculate the contributions from the s -channel diagrams to the reaction densities analytically in the limit $c_j \rightarrow 0$, while the contributions from the t -channel diagrams can easily be calculated numerically.

D.2 Interactions with quarks and squarks

The reaction densities $\gamma_{t_j}^{(i)}$ for the interaction of a (s)neutrino with a top or a stop can also be calculated analytically in the limit of high temperatures $z \ll 1/\sqrt{a_j}$. For the s -channel processes one finds

$$\gamma_{t_j}^{(0)} = \frac{3\alpha_u M_1^4}{64\pi^4} (\lambda_\nu^\dagger \lambda_\nu)_{jj} a_j \frac{K_2(z\sqrt{a_j})}{z^2} , \quad (\text{D.16})$$

$$\gamma_{t_j}^{(3)} = 2\gamma_{t_j}^{(0)} , \quad \gamma_{t_j}^{(5)} = \gamma_{t_j}^{(0)} . \quad (\text{D.17})$$

For the t -channel reaction densities one has analogously

$$\gamma_{t_j}^{(1)} = \frac{3\alpha_u M_1^4}{8\pi^4} (\lambda_\nu^\dagger \lambda_\nu)_{jj} \frac{1}{z^4} \left[\left(1 - \frac{z^2 a_j}{4}\right) K_0(z\sqrt{a_j}) + \frac{z^2 a_j}{4} \left(\ln\left(\frac{a_j}{a_h}\right) - 1\right) K_2(z\sqrt{a_j}) \right] , \quad (\text{D.18})$$

$$\gamma_{t_j}^{(2)} = \frac{3\alpha_u M_1^4}{8\pi^4} (\lambda_\nu^\dagger \lambda_\nu)_{jj} \frac{1}{z^4} \left[\left(1 - \frac{z^2 a_j}{4}\right) K_0(z\sqrt{a_j}) + \frac{z^2 a_j}{4} \ln\left(\frac{a_j}{a_h}\right) K_2(z\sqrt{a_j}) \right] , \quad (\text{D.19})$$

$$\gamma_{t_j}^{(4)} = 2\gamma_{t_j}^{(0)} , \quad \gamma_{t_j}^{(6)} = \gamma_{t_j}^{(1)} , \quad \gamma_{t_j}^{(7)} = \gamma_{t_j}^{(2)} . \quad (\text{D.20})$$

$\gamma_{t_j}^{(8)}$ and $\gamma_{t_j}^{(9)}$ are several orders of magnitude smaller than the other $\gamma_{t_j}^{(i)}$ for small z and can therefore be neglected at high temperatures.

By using the series expansions of the Bessel functions, one sees that the processes with a higgsino in the t -channel, i.e. $\gamma_{t_j}^{(1)}$, $\gamma_{t_j}^{(2)}$, $\gamma_{t_j}^{(6)}$ and $\gamma_{t_j}^{(7)}$, behave like $T^4 \ln(T/M_j)$ at high temperatures, whereas the other reaction densities are proportional to T^4 .

D.3 Pair creation and annihilation of neutrinos

In the Boltzmann equations we only need certain combinations of reaction densities which can easily be evaluated for high temperatures:

$$\begin{aligned} \sum_{k=1}^2 \gamma_{N_i N_j}^{(k)} &= \sum_{k=1}^2 \gamma_{\widetilde{N}_i^c \widetilde{N}_j^c}^{(k)} = \gamma_{N_j \widetilde{N}_i^c}^{(1)} = \\ &= \frac{M_1^4}{16\pi^5} \frac{1}{z^4} (\lambda_\nu^\dagger \lambda_\nu)_{jj} (\lambda_\nu^\dagger \lambda_\nu)_{ii} \left\{ \left[1 - \frac{z^2}{4} (\sqrt{a_i} + \sqrt{a_j})^2 \right] K_0(z(\sqrt{a_i} + \sqrt{a_j})) \right\} \end{aligned} \quad (\text{D.21})$$

$$\begin{aligned}
& + \frac{z^2}{4} (\sqrt{a_i} + \sqrt{a_j})^2 \left[1 + \ln \left(2 + \frac{a_i + a_j}{\sqrt{a_i a_j}} \right) \right] K_2 \left(z (\sqrt{a_i} + \sqrt{a_j}) \right) \Big\} , \\
\sum_{k=3}^4 \gamma_{N_i N_j}^{(k)} &= \sum_{k=3}^4 \widetilde{\gamma_{N_i^c N_j^c}^{(k)}} = \gamma_{N_j N_i^c}^{(2)} = \\
&= \frac{M_1^4}{16\pi^5} \frac{1}{z^4} \left| (\lambda_\nu^\dagger \lambda_\nu)_{jj} \right|^2 \left\{ \left[1 - \frac{z^2}{4} (\sqrt{a_i} + \sqrt{a_j})^2 \right] K_0 \left(z (\sqrt{a_i} + \sqrt{a_j}) \right) \right. \\
&\quad \left. + \frac{z^2}{4} (\sqrt{a_i} + \sqrt{a_j})^2 \left[1 + \ln \left(2 + \frac{a_i + a_j}{\sqrt{a_i a_j}} \right) \right] K_2 \left(z (\sqrt{a_i} + \sqrt{a_j}) \right) \right\} ,
\end{aligned} \tag{D.22}$$

i.e. these reaction densities are proportional to $T^4 \ln(T/(M_i + M_j))$ at high temperatures.

References

- [1] For a review and references, see E. W. Kolb and M. S. Turner, *The Early Universe*, (Addison-Wesley, Redwood City, CA, 1990)
- [2] For a recent review, see R. H. Brandenberger, *Particle Physics Aspects of Modern Cosmology*, to be published in *Field Theoretical Methods in Fundamental Physics*, ed. by Choonyu Lee, Mineumsa Co. Ltd., Seoul, 1997, Preprint BROWN-HET-1067, hep-ph/9701276
- [3] For a discussion and references, see V. A. Rubakov and M. E. Shaposhnikov, Phys. Usp. **39** (1996) 461;
- [4] For a discussion and references, see K. Jansen, Nucl. Phys. B (Proc. Supp.) 47 (1996) 196
- [5] V. A. Kuzmin, V. A. Rubakov and M. E. Shaposhnikov, Phys. Lett. **B 155** (1985) 36
- [6] T. Yanagida, in: *Workshop on unified Theories*, KEK report 79-18 (1979) p. 95;
M. Gell-Mann et al., in: *Supergravity*, Proc. of the Stony Brook Workshop 1979, eds. P. van Nieuwenhuizen and D. Freedman (North Holland, Amsterdam, 1979), p. 315
- [7] M. Fukugita and T. Yanagida, Phys. Lett. **B 174** (1986) 45
- [8] P. Langacker, R. D. Peccei and T. Yanagida, Mod. Phys. Lett. **A 1** (1986) 541;
T. Gherghetta and G. Jungman, Phys. Rev. **D 48** (1993) 1546;
M. Flanz, E. A. Paschos and U. Sarkar, Phys. Lett. **B 345** (1995) 248, *ibid.* **B 384** (1996) 487 (E);
M. Flanz, E. A. Paschos, U. Sarkar and J. Weiss, Phys. Lett. **B 389** (1996) 693;
M. P. Worah, Phys. Rev. **D 53** (1996) 3902;
L. Covi and E. Roulet, Phys. Lett. **B 399** (1997) 113
- [9] M. A. Luty, Phys. Rev. **D 45** (1992) 455

- [10] B. A. Campbell, S. Davidson and K. A. Olive, Nucl. Phys. **B 399** (1993) 111
- [11] M. Plümacher, Z. Phys. **C 74** (1997) 549
- [12] W. Buchmüller and M. Plümacher, Phys. Lett. **B 389** (1996) 73
- [13] L. Covi, E. Roulet and F. Vissani, Phys. Lett. **B 384** (1996) 169
- [14] A. D. Dolgov and Ya. B. Zeldovich, Rev. Mod. Phys. **53** (1981) 1;
E. W. Kolb and S. Wolfram, Nucl. Phys. **B 172** (1980) 224, *ibid.* **B 195** (1982) 542 (E)
- [15] W.-Y. Keung and L. Littenberg, Phys. Rev. **D 28** (1983) 1067
- [16] S. Yu. Khlebnikov and M. E. Shaposhnikov Nucl. Phys. **B 308** (1988) 885
- [17] L. E. Ibáñez and F. Quevedo, Phys. Lett. **B 283** (1992) 261
- [18] L. Wolfenstein, Phys. Rev. Lett. **51** (1983) 1945
- [19] L. Wolfenstein, Phys. Rev. **D 17** (1978) 2369;
S. P. Mikheyev and A. Y. Smirnov, Nuovo Cim. **9C** (1986) 17
- [20] W. C. Haxton, Annu. Rev. Astron. Astrophys., **33** (1995) 459
- [21] E. Witten, Phys. Lett. **B 91** (1980) 81;
Z. Berezhiani, in: *High Energy Physics and Cosmology*, Proc. of the 1995 ICTP Summer School, Trieste, eds. E. Gava, A. Masiero and K. S. Narain (World Scientific, Singapore, 1997), p. 618
- [22] H. Murayama and T. Yanagida, Phys. Lett. **B 322** (1994) 349;
M. Dine, L. Randall and S. Thomas, Nucl. Phys. **B 458** (1996) 291;
G. Lazarides, R. K. Schaefer and Q. Shafi, Phys. Rev. **D 56** (1997) 1324
- [23] J. Wess and J. Bagger, *Supersymmetry and Supergravity*, (Princeton University Press, Princeton, NJ, 1992)